Differentiation of a Gabbro Sill in the Oregon Coast Range by Crystallization-Zone Settling

GEOLOGICAL SURVEY PROFESSIONAL PAPER 1165

Differentiation of a Gabbro Sill in the Oregon Coast Range by Crystallization-Zone Settling

By NORMAN S. MacLEOD

GEOLOGICAL SURVEY PROFESSIONAL PAPER 1165

UNITED STATES GOVERNMENT PRINTING OFFICE, WASHINGTON: 1981

UNITED STATES DEPARTMENT OF THE INTERIOR

JAMES G. WATT, ***Secretary***

GEOLOGICAL SURVEY

Doyle G. Frederick, ***Acting Director***

Library of Congress catalog-card No. 81-600049

For sale by the Superintendent of Documents, U.S. Government Printing Office
Washington, D.C. 20402

CONTENTS

ILLUSTRATIONS

TABLES

DIFFERENTIATION OF A GABBRO SILL IN THE OREGON COAST RANGE BY CRYSTALLIZATION-ZONE SETTLING

By Norman S. MacLeod

ABSTRACT

At Stott Mountain in the Oregon Coast Range, an iron-rich granophyric gabbro sill, 90 to 229 m thick, is strongly differentiated but shows no rhythmic layering or crystal lamination. Gabbro in the lower half is progressively more mafic upward from the base to the center of the sill. Above the center the rocks are progressively more felsic, and ferrogranophyre and granophyre are abundant. At the top of the sill, gabbro like that near the base forms a thin zone below the upper chilled margin. The bulk composition of the sill and the composition of the chilled margins are virtually identical. Thus differentiation occurred in place without significant assimilation of country rock or influxes of magma of different composition.

Differentiation probably resulted from settling of crystals that were precipitating in two zones that moved inward from the bottom and top of the sill as it solidified. In the lower zone, crystals formed over a thermal gradient and settled according to their height of nucleation within the zone and their density and size. As the lower crystallization zone progressed continuously upward, differentiation became progressively more pronounced because the thermal gradient within the zone decreased, consequently increasing the thickness of the zone and the time available for settling. The minerals changed composition upward because an increasingly greater proportion of relatively silicic residual liquid was displaced upward out of the lower zone and thus was not available for reaction. In the upper zone crystals also settled, but they were apparently resorbed as they passed into the higher temperature liquid interior of the sill. The ferrogranophyre and granophyre in the upper part of the sill formed from late residual magma.

INTRODUCTION

A gabbro sill in the central part of the Oregon Coast Range contains rocks that range widely in composition; for example, their SiO_2 content ranges from 51 to 76 percent, and Fe_2O_3+FeO from 2 to 18 percent. The bulk composition of the sill is nearly the same as that of the chilled margins; thus differentiation must have occurred in place. The chemical, modal, and mineralogic composition of rocks collected at intervals in the lower half show that the sill is progressively more mafic upward from the base to the center. This part of the sill is massive with no crystal layering or lamination, and rock textures are not obviously cumulate. Nevertheless, the cryptic vertical change in composition appears to be the result of crystal settling. In succeeding sections of this report the petrography, mineralogy, and textures of the rocks, the order of crystallization of the minerals, and the vertical modal, mineralogic, and chemical variations are described. In the last section they are shown to be consistent with differentiation by crystal settling within crystallization zones that moved progressively toward the sill's interior as it cooled and solidified.

This report is a product of geologic mapping and petrochemical studies of volcanic and intrusive rocks of the Oregon Coast Range carried out by P. D. Snavely, Jr., and the author. Snavely kindly made available several chemical analyses of the gabbro sill which he obtained prior to this study, as well as analyses of related sills farther south. I am indebted to him for providing the opportunity for this study and for his encouragement and advice.

GEOLOGIC SETTING

Granophyric gabbro sills underlie many of the higher mountains in a 5,000-km^2 area of the Oregon Coast Range between lat 43°45′ N. and 45° N. (Snavely and Wagner, 1961; Baldwin, 1964; Snavely and others, 1976). Three K-Ar ages on minerals from these sills range from 29.9 to 31.6 million years (Tatsumoto and Snavely, 1969; P. D. Snavely, Jr., unpub. data) and indicate an Oligocene age. The sills are typically 120 to 170 m thick; the thickest, at Marys Peak, near Corvallis, Oreg., is about 335 m (Roberts, 1953; Baldwin, 1955; Clark, 1969).

The granophyric gabbro sill near Stott Mountain, the subject of this report, is the northernmost of this group of sills (MacLeod, 1969). It was formerly more widespread, but now crops out only as erosional remnants on higher ridges and peaks in the Valsetz and Euchre Mountain 15-minute quadrangles (fig. 1). No feeder dikes were found near Stott Mountain, but two large dikes to the south (fig. 1) are similar in composition to the Stott sill and either may formerly have been connected to it.

The gabbro sill intrudes sandstone and siltstone of

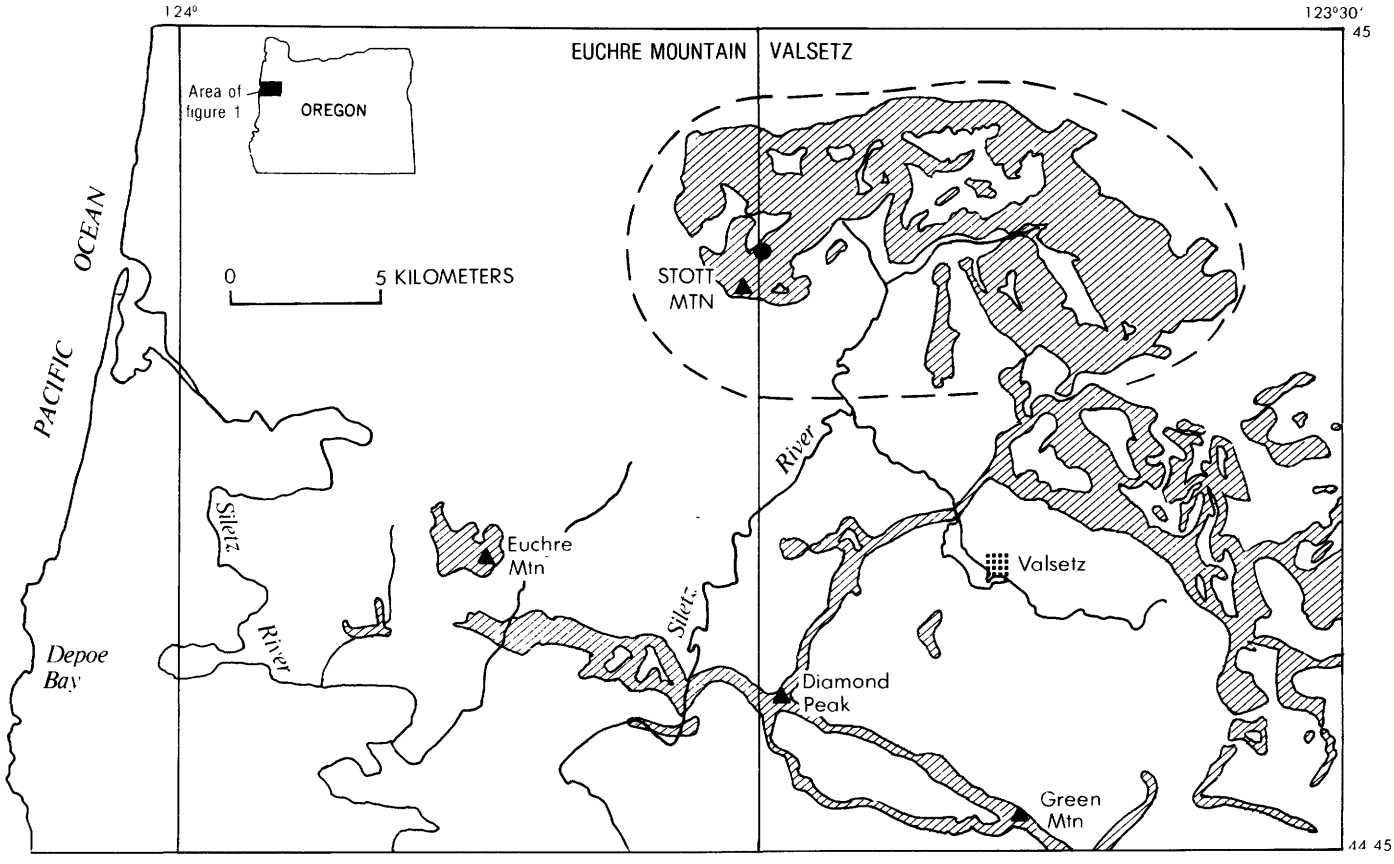

Figure 1. Distribution (cross-hatched areas) of Oligocene gabbro sills, dikes, and inclined sheets in Euchre Mountain (Snavely and others, 1976) and Valsetz (Baldwin, 1964; MacLeod, 1969) 15-minute quadrangles, Oregon. Dashed line outlines Stott Mountain sill; dikes and inclined sheets that may have fed Stott sill trend west-northwest and north-northeast from Diamond Peak. Solid circle shows location of samples described in table 1.

the middle Eocene Tyee Formation and siltstone with interbedded tuff, basaltic sandstone, and glauconitic sandstone of the Yamhill Formation of middle and early late Eocene age. These deep-water marine sedimentary rocks overlie basalt breccias, pillow flows, tuffs, and massive flows of the lower and middle Eocene Siletz River Volcanics, which are the oldest rocks exposed in the Coast Range (Snavely and others, 1968).

The Stott Mountain sill ranges in thickness from 90 to about 220 m; several small sills, less than 1 m to about 45 m thick, occur in a few places above and below the main sill. Locally the sill becomes an inclined sheet with discordance to sedimentary bedding of 5° or more.

The sedimentary rocks are baked as far as 10 m from the sill. Hornfels with incipient andalusite and, less commonly, cordierite porphyroblasts have resulted from baking of siltstone in a few places; sandstone appears bleached, but only its matrix minerals are recrystallized. No evidence of assimilation of these sedimentary rocks was found within the sill.

GENERAL FEATURES

The chilled borders of the sill range from 0.5 m to 3 m in thickness. The chilled basalt grades inward to fine- and medium-grained gabbro. The interior of the sill is divided into three intergradational zones (fig. 2). The thick lower and thin upper gabbro zones are separated by a silicic zone composed of ferrogranophyre, granophyre, and pegmatite. The sill was systematically sampled from base to top along a small ravine on the north side of Stott Mountain (fig. 1) where the sill is about 140 m thick. Here the lower gabbro zone is about 98 m thick, the silicic zone, about 35 m, and the upper gabbro zone is about 7 m thick.

Gabbro in the lower and upper zones is massive in appearance. Field and thin-section studies show that it is not rhythmically layered and that it lacks crystal lamination.

The silicic zone is heterogeneous. It is composed

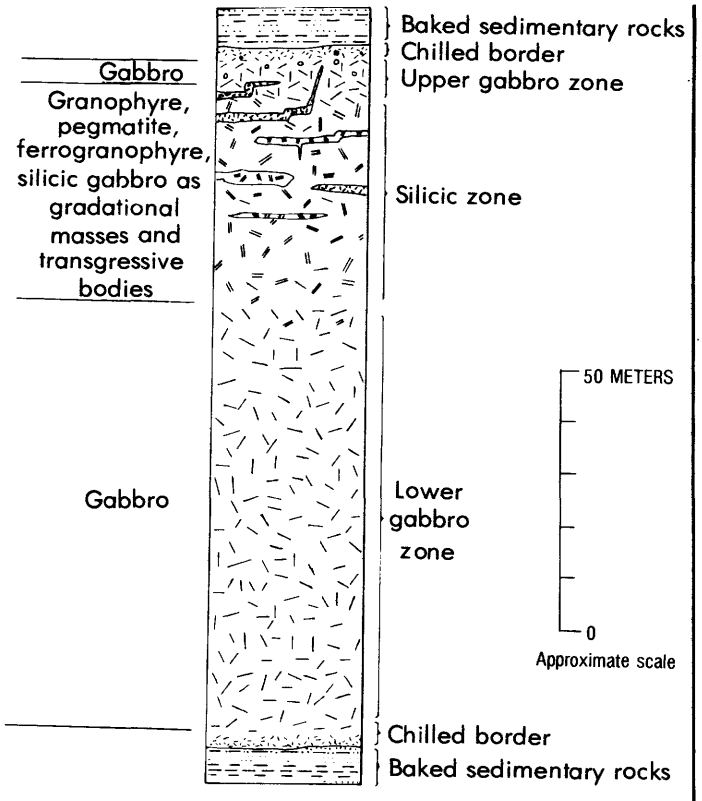

Figure 2. Distribution of rock types in gabbro sill.

principally of ferrogranophyre but also contains granophyre, pegmatite, and silicic gabbro. Transgressive bodies composed of ferrogranophyre, granophyre, and pegmatite occur in the upper part of the silicic zone, and some extend into the upper gabbro zone. Most of the transgressive bodies parallel the upper contact of the sill, extend laterally less than 50 m, and are 2–10 m thick. In detail they are very irregular and commonly bifurcate. Contacts of the bodies with the enclosing rock are sharp but show no evidence of chilling. The transgressive bodies are interpreted as resulting from injection of late residual magma produced by differentiation within the sill into its upper part. The limited horizontal extent of individual bodies suggests that the residual magma was derived nearby.

PETROGRAPHY

CHILLED BASALT

The chilled borders of the sill are composed of dark-gray very fine grained basalt. The grain size gradually increases from less than 0.1 mm for larger crystals at the contact to about 1 mm at 3 m from the contact. The chilled basalt has an intersertal or intergranular and variolitic texture. Most is aphyric, but some contains rare plagioclase microphenocrysts less than 1 mm long. The chilled basalt is composed of fine radiating sheaves of plagioclase and minute grains of titaniferous ferroaugite, actinolite, biotite, opaque minerals, and clay minerals.

The chilled basalt is extensively altered. Plagioclase is clouded with fine-grained albite, chlorite, and (or) clay minerals that surround a few remaining relict patches of primary sodic labradorite. Former glass(?) is replaced by clay minerals, actinolite, and biolite.

GABBRO

The mafic rocks that form the bulk of the the sill are not readily classified and are here called gabbro to avoid a cumbersome nomenclature. The SiO_2 content of 51 to 59 percent is greater than that of most gabbros, but the rocks have an unusually high iron content (13 to 18 percent as FeO) that results in a color index between 30 and 40, and the plagioclase is mostly labradorite. Similar rocks from other areas have been variously called ferrogranophyre, granophyre, granophyric ferrodiabase, quartz dolerite, or leucogabbro.

The gabbro is medium dark gray and weathers to light gray or reddish brown. Grain size is typically 0.3–1 mm, and the largest crystals are as much as 3 mm across. The average grain size increases only slightly from the base toward the sill center. The texture is granophyric and hypidiomorphic-granular and locally slightly subophitic. The gabbro in both the lower and upper zones is massive, and neither layering nor crystal lamination is present. The gabbro changes composition vertically, as discussed later, but this variation is not obvious in the field.

The gabbro is composed of plagioclase, ferroaugite, iron-rich olivine, apatite, and opaque minerals surrounded by quartz and alkali feldspar (both as intergrowths and isolated crystals) and patches of phyllosilicate minerals (tables 1 and 2). Iron-rich hornblende locally occurs as overgrowths on ferroaugite; it is also associated with iron-rich nontronitic clay minerals, biotite, and chlorite which together form the phyllosilicate patches.

Olivine occurs in equilibrium with quartz in the gabbro as well as in all other rocks from the sill because it has a very high iron content (fo_{19-2}). Olivine also occurs with quartz in late-stage rocks of the Skaergaard intrusion, Greenland (Wager and Brown, 1968) and quartz-Fe-olivine-Ca-Fe-clinopyroxene are stable coexisting phases at moderately low pressure (Smith, 1971).

FERROGRANOPHYRE

The ferrogranophyre is mottled medium gray or brownish gray and is lighter colored than gabbro,

TABLE 1.—*Modal, mineralogical, and chemical*

MODAL ANALYSES												
Height above base of sill (meters) --	4-1/2	9	13-1/2	24-1/2	29	35	42-1/2	49	62-1/2	70	81	91
Rock number -------	M203	M204	M205	M206	M207	M208	M209	M210	M211	M212	M213	M214
Plagioclase -------	33.0	32.6	36.0	35.2	34.9	36.6	37.2	37.2	36.3	39.4	38.7	33.0
Q-F intergrowth[2] --	27.6	27.8	24.9	24.6	21.4	21.8	20.6	19.0	17.2	16.7	17.8	21.8
Quartz[2] ----------	2.9	2.9	2.3	3.4	5.1	3.7	2.6	3.2	2.9	3.0	2.9	4.3
Alkali feldspar[2] --	1.7	1.7	1.1	2.1	3.0	1.5	1.5	1.3	2.2	1.6	1.9	4.7
Apatite ----------	.8	.6	.7	.9	1.3	1.2	1.3	1.4	1.6	1.6	1.7	2.0
Pyroxene ---------	9.6	10.2	9.9	10.4	10.1	10.0	10.0	9.9	10.7	9.8	9.5	6.7
Olivine ----------	10.3	9.5	11.3	10.2	11.6	11.7	11.6	12.9	13.8	12.5	12.4	11.5
Opaque minerals ---	2.2	2.2	2.9	3.0	2.9	3.3	3.3	3.2	3.7	4.3	4.0	3.7
Hornblende --------	.3	1.6	2.0	1.5	1.4	1.7	1.1	.1	.4	.2	.6	.7
Phyllosilicates ---	11.6	10.9	8.9	8.7	8.3	8.5	10.8	11.8	12.2	10.8	11.5	11.4
Color index -------	34.0	34.4	35.0	33.8	34.3	35.2	36.8	37.9	40.8	37.7	38.0	34.0
MINERAL DATA												
Olivine (percent fo)	13.	-	12.	17.	18.	-	17.	18.	18.	18.	19.	19.
Pyroxene: Ny ------	1.721	1.721	1.721	1.721	1.721	1.721	1.720	1.720	1.720	1.720	1.719	1.719
Pyroxene: 2V ------	52.	51.	52.	50.	51.	51.	52.	51.	51.	52.	52.	50.
Plagioclase (percent an in cores) -------	51.	51.	54.	54.	56.	55.	54.	51.	54.	54.	54.	54.
CHEMICAL ANALYSES (RECALCULATED H_2O-FREE TO 100 PERCENT)												
SiO_2 ----------	57.6	57.5	56.9	55.4	55.4	55.0	54.7	53.7	53.5	53.6	52.0	54.6
Al_2O_3 ----------	13.5	13.3	13.4	13.7	13.2	13.2	13.3	13.4	12.9	13.5	13.1	13.4
Fe_2O_3 ----------	2.9	2.6	1.4	2.3	2.3	3.2	3.3	3.6	3.0	3.7	2.7	3.8
FeO ----------	11.5	11.9	13.0	13.4	13.2	12.9	12.8	12.7	13.7	13.6	15.3	12.5
MgO ----------	1.4	1.4	1.6	1.6	2.0	1.9	2.1	2.1	2.2	2.2	2.3	1.9
CaO ----------	6.0	6.1	6.5	6.5	6.8	6.8	7.0	7.3	7.5	7.2	7.3	6.9
Na_2O ----------	2.9	3.0	2.7	2.7	2.7	2.6	2.5	2.7	2.7	2.8	2.5	2.6
K_2O ----------	1.9	1.5	1.7	1.3	1.5	1.5	1.4	1.3	1.3	1.0	1.2	1.4
TiO_2 ----------	1.5	1.7	1.7	1.8	1.8	1.9	1.9	2.0	2.0	1.6	2.3	1.9
P_2O_5 ----------	.67	.72	.73	.93	.85	.83	.87	.88	.86	.68	1.0	.85
MnO ----------	.27	.26	.28	.29	.30	.29	.31	.30	.32	.20	.33	.30

TABLE 2.—*Chemical analyses and*

	Lower zone gabbro	Upper zone gabbro			Silicic zone										
					Gabbro			Ferrogranophyre			Pegmatite		Granophyre		
Column number ----	1	2	3	4	5	6	7	8	9	10	11	12	13	14	15
Rock number ------	61-66	60-56	66-124	66-125	67-216	67-218	67-219	66-145	60-62	67-215	66-144	66-136	61-65	66-142	66-135
MODAL ANALYSES															
Plagioclase ------	33	41	34	34	41	35	31	34	31	29	32	33	(too fine grained		10
Q-F intergrowth --	24	22	27	26	19	28	32	38	30	26	45	29	to determine		86
Quartz ----------	3	2	3	2	4	4	3	3	7	8	7	2	mode)		-
Alkali feldspar --	1	1	2	2	3	3	3	4	3	10	2	7			-
Apatite ----------	1	1	1	1	2	1/2	1/2	-	-	-	-	1/2			-
Pyroxene ---------	13	11	9	10	9	10	10	6	10	8	5	6			2
Olivine ----------	9	8	9	7	6	8	12	7	5	2	5	2			-
Opaque minerals --	3	3	2	5	2	3	2	2	2	2	1	5			1/2
Hornblende -------	1	1	2	1	1	2	1/2	1	-	3	1	1/2			-
Phyllosilicates --	12	10	11	12	12	7	7	5	12	12	2	6			2
Color index ------	38	33	33	35	30	29	31	21	29	26	14	19			4
MINERAL DATA															
Olivine (percent fo)	-	-	-	-	16	15	10	9	-	-	4	-			-
Pyroxene: Ny -----	1.718	1.722	-	1.723	1.722	1.724	1.723	1.734	1.725	1.724	1.737	1.735-8			1.739
Pyroxene: 2V -----	51.	50.	-	50.	51.	52.	50.	54.	53.	51.	54.	52-56			55.
Plagioclase (percent An in cores) ------	53.	54.	54.	54.	54.	51.	-	51.	45.	-	51.	-			2.
CHEMICAL ANALYSES (RECALCULATED WATER-FREE TO 100 PERCENT)															
SiO_2 ----------	51.7	54.7	55.5	55.7	56.6	57.7	59.2	60.6	61.2	63.1	63.4	65.7	72.4	74.9	76.1
Al_2O_3 ----------	13.1	12.9	13.9	13.3	14.9	13.3	13.3	13.6	13.0	13.4	13.4	14.3	13.9	13.0	12.6
Fe_2O_3 ----------	4.1	3.3	3.4	3.0	4.0	3.3	3.5	2.7	5.6	4.0	5.3	1.8	1.8	2.7	.38
FeO ----------	14.3	13.2	11.9	12.3	9.3	11.1	10.2	9.8	7.6	7.7	5.8	5.4	1.9	.53	1.2
MgO ----------	1.9	1.2	1.6	1.7	1.3	1.4	1.1	.93	.49	.68	.53	.49	.27	.05	.11
CaO ----------	6.6	7.0	6.7	6.9	6.7	6.2	5.9	5.4	4.5	4.4	4.6	3.8	.54	.33	.76
Na_2O ----------	2.7	2.9	2.6	2.7	3.1	2.7	2.8	3.0	3.1	3.0	3.4	5.4	6.2	3.5	4.1
K_2O ----------	1.5	1.5	1.6	1.5	1.6	1.7	1.9	2.2	2.1	2.2	2.5	2.0	2.4	4.1	4.3
TiO_2 ----------	2.7	2.2	2.1	2.1	1.6	1.7	1.4	1.3	1.5	1.0	.81	.84	.37	.29	.31
P_2O_5 ----------	1.0	.85	.67	.76	.61	.67	.57	.40	.58	.32	.26	.17	.04	.00	.02
MnO ----------	.35	.32	.23	.22	.27	.29	.26	.17	.25	.23	.14	.04	.06	.09	.06

data for rocks from the lower gabbro zone

Height above base of sill (meters)	4-1/2	9	13-1/2	24-1/2	29	35	42-1/2	49	62-1/2	70	81	91
Rock number	M203	M204	M205	M206	M207	M208	M209	M210	M211	M212	M213	M214
MODAL ANALYSES												
Q	12.6	13.4	12.9	11.8	10.7	10.5	10.5	8.4	7.8	7.5	7.1	10.1
or	11.2	8.9	10.0	7.7	8.9	8.9	8.3	7.7	7.7	5.9	7.1	8.3
ab	24.5	25.4	22.8	22.8	22.8	22.0	21.2	22.8	22.8	23.7	21.2	22.0
an	18.2	18.4	19.4	21.4	19.5	19.9	20.9	20.6	19.2	21.3	21.0	20.8
di: wo	3.0	3.0	3.4	2.2	3.7	3.5	3.4	4.1	5.2	4.2	3.7	3.3
di: en	.5	.5	.6	.4	.7	.7	.7	.8	1.0	.8	.7	.6
hy: fs	2.8	2.8	3.1	2.0	3.2	3.1	3.0	3.6	4.5	3.7	3.2	3.0
hy: en	3.0	3.0	3.4	3.6	4.3	4.1	4.5	4.4	4.4	4.7	5.0	4.1
hy: fs	17.8	17.6	17.4	20.2	18.7	19.5	19.7	19.2	19.0	21.2	21.9	20.0
mt	2.1	2.1	2.0	2.3	2.2	2.3	2.3	2.4	2.4	2.5	2.6	2.4
il	2.8	3.2	3.2	3.4	3.4	3.6	3.6	3.8	3.8	3.0	4.4	3.6
ap	1.6	1.7	1.7	2.2	2.0	2.0	2.1	2.1	2.0	1.6	2.4	2.0
CHEMICAL ANALYSES (ORIGINAL)[3]												
SiO_2	56.1	55.7	55.5	54.3	54.1	53.6	53.1	52.0	51.7	51.3	50.7	53.0
Al_2O_3	13.1	12.9	13.1	13.4	12.9	12.9	12.9	13.0	12.5	12.9	12.8	13.0
Fe_2O_3	2.8	2.5	1.4	2.2	2.2	3.1	3.2	3.5	2.9	3.5	2.6	3.7
FeO	11.2	11.5	12.7	13.1	12.9	12.6	12.4	12.3	13.2	13.0	14.9	12.1
MgO	1.4	1.4	1.6	1.6	1.9	1.8	2.0	2.0	2.1	2.1	2.2	1.8
CaO	5.8	5.9	6.3	6.5	6.6	6.6	6.8	7.1	7.2	6.9	7.1	6.7
Na_2O	2.8	2.9	2.6	2.6	2.6	2.5	2.4	2.6	2.6	2.7	2.4	2.5
K_2O	1.8	1.5	1.7	1.3	1.5	1.5	1.4	1.3	1.2	1.0	1.2	1.4
H_2O-	1.2	1.3	1.1	.91	.92	1.2	1.4	1.4	1.3	1.5	1.1	1.4
H_2O+	1.4	1.3	1.2	1.1	1.3	1.3	1.3	1.6	1.9	2.0	1.3	1.4
TiO_2	1.5	1.6	1.7	1.8	1.8	1.8	1.8	1.9	2.1	1.5	2.2	1.8
P_2O_5	.65	.70	.71	.91	.83	.81	.85	.85	.83	.65	1.0	.83
MnO	.26	.25	.27	.28	.29	.28	.30	.29	.31	.19	.32	.29
Total	100.0	99.5	99.9	100.0	99.8	100.0	99.9	99.8	99.8	99.2	99.8	99.9

[1]Samples collected along small ravine in center sec. line 25-26, T. 7 S., R. 9 W., Valsetz 15' quadrangle.

[2]Individual quartz and alkali feldspar and intergrown quartz and feldspar counted separately.

[3]Chemical analyses were made by S. Botts, H. Smith, G. Chloe, L. Artis, J. Kelsey, J. Glenn, P. Elmore, and I. Barlow using methods described in U.S. Geological Survey Bulletin 1144A, supplemented by atomic absorption. Modal analyses are based on 2,000 points or more per sample end an additional 2,000 points for opaque minerals and apatite.

norms of rocks from the gabbro sill

	Lower zone gabbro	Upper zone gabbro			Silicic zone										
					Gabbro			Ferrogranophyre			Pegmatite		Granophyre		
Column number	1	2	3	4	5	6	7	8	9	10	11	12	13	14	15
Rock number	61-66	60-56	66-124	66-125	67-216	67-218	67-219	66-145	60-62	67-215	66-144	66-136	61-65	66-142	66-135
NORMS (CALCULATED WITH Fe_2O_3 = 10 PERCENT TOTAL Fe)															
Q	6.2	9.7	11.4	11.6	10.9	14.3	15.6	16.3	18.6	20.6	18.3	15.6	[2]23.3	[3]35.9	33.2
or	8.9	8.9	9.5	8.9	9.5	10.1	11.2	13.0	12.4	13.0	14.8	11.8	14.2	24.2	25.4
ab	22.9	24.5	22.0	22.9	26.2	22.9	23.7	25.4	26.2	25.4	28.8	45.7	52.5	29.6	34.7
an	19.2	17.8	21.5	19.7	22.0	19.2	18.1	17.1	15.4	16.6	13.9	8.9	2.4	1.6	3.3
di: wo	3.0	4.8	3.1	4.0	3.0	3.0	3.1	3.0	1.3	1.3	3.0	3.7	-	-	.2
di: en	0.5	0.6	0.5	0.7	0.5	0.5	0.4	0.4	0.1	0.1	0.3	0.4	-	-	-
hy: fs	2.7	4.7	2.8	3.6	2.8	2.8	3.0	2.9	1.4	1.3	3.1	3.6	-	-	.2
hy: en	4.2	2.4	3.5	3.5	2.8	3.0	2.3	1.9	1.1	1.6	1.1	.8	.7	.1	.3
hy: fs	22.4	18.2	18.3	17.4	15.9	17.5	16.7	14.9	17.3	15.8	13.3	6.4	5.3	4.8	1.9
mt	2.7	2.4	2.2	2.2	1.9	2.1	2.0	1.8	1.9	1.7	1.6	1.0	.5	.5	.2
il	5.1	4.2	4.0	4.0	3.0	3.2	2.7	2.5	2.9	1.9	1.5	1.6	.7	.6	.6
ap	2.4	2.0	1.6	1.8	1.4	1.6	1.3	1.0	1.4	.8	.6	.4	.1	-	.1
CHEMICAL ANALYSES (ORIGINAL)[1]															
SiO_2	50.0	53.2	53.7	53.6	54.8	56.0	57.5	59.0	58.8	61.3	61.6	64.5	72.0	73.1	75.3
Al_2O_3	12.7	12.5	13.4	12.8	14.4	12.9	12.9	13.2	12.5	13.0	13.0	14.0	13.8	13.3	12.5
Fe_2O_3	4.0	3.2	3.3	2.9	3.9	3.2	3.4	2.6	5.4	3.9	5.1	1.8	1.8	2.6	.38
FeO	13.8	12.8	11.5	11.8	9.0	10.8	9.9	9.5	7.3	7.5	5.6	5.3	1.9	.52	1.2
MgO	1.8	1.2	1.5	1.6	1.3	1.4	1.1	.91	.47	.66	.52	.48	.27	.05	.11
CaO	6.4	6.8	6.5	6.6	6.5	6.0	5.7	5.3	4.3	4.3	4.5	3.7	.54	.52	.75
Na_2O	2.6	2.8	2.5	2.6	3.0	2.6	2.7	2.9	3.0	2.9	3.3	5.3	6.2	3.4	4.1
K_2O	1.4	1.5	1.5	1.4	1.5	1.6	1.8	2.1	2.0	2.1	2.4	2.0	2.4	4.0	4.2
H_2O-	1.3	1.2	1.2	1.3	1.5	1.5	1.3	.79	1.4	1.2	1.0	.59	.41	.81	.16
H_2O+	1.7	1.0	2.0	2.0	1.6	1.3	1.1	1.7	2.0	1.4	1.8	1.2	.85	1.6	.69
TiO_2	2.6	2.1	2.0	2.0	1.5	1.6	1.4	1.3	1.4	1.0	.79	.82	.37	.28	.31
P_2O_5	1.0	.83	.65	.73	.59	.65	.55	.39	.56	.31	.25	.17	.04	.00	.02
MnO	.34	.31	.22	.21	.26	.28	.25	.17	.24	.22	.14	.04	.06	.09	.06
Total	99.6	99.4	100.0	99.5	99.9	99.8	99.6	99.9	99.4	99.8	100.0	99.9	100.6	100.3	99.8

[1]Chemical analyses were made by S. Botts, H. Smith, G. Chloe, L. Artis, J. Kelsey, J. Glenn, P. Elmore, and I. Barlow using methods described in U.S. Geological Survey Bulletin 1144A, supplemented by atomic absorption.
[2]C = 0.2.
[3]C = 2.2.

owing largely to the greater abundance of interstitial quartz and alkali-feldspar. Grain size is variable even in individual samples, but larger crystals are typically 1-3 mm long. The rock is composed of the same minerals as the gabbro but in different proportions (table 2). Because of the greater abundance of late-formed granophyric intergrowths of quartz and alkali-feldspar, crystals of plagioclase, pyroxene, and olivine tend to be more euhedral than in gabbro.

Plagioclase is less abundant in the ferrogranophyre than in the gabbro. Crystal-core compositions are similar, but progressively zoned rims are larger in the ferrogranophyre and the bulk plagioclase is more sodic. Olivine and apatite are also less abundant than in gabbro, but the content of opaque minerals and hornblende is about the same. Variable amounts of phyllosilicates (iron-rich clay minerals, chlorite, and biotite) occur with quartz-feldspar intergrowth. Olivine is fayalitic, and the pyroxene is ferroaugite or ferrohedenbergite.

PEGMATITE

Small bodies of pegmatite, a coarse-grained (as large as 5 cm) variety of ferrogranophyre, occur within the silicic zone. They form masses that grade into ferrogranophyre and also form transgressive bodies. Some pegmatite contains as much as 17 percent olivine, but most contains less than 7 percent. Olivine and ferroaugite are very rich in iron (table 2). Plagioclase displays marked progressive zoning and ranges from sodic labradorite or andesine in crystal cores to calcic oligoclase on the rims.

GRANOPHYRE

Granophyre, which constitutes less than 5 percent of the sill, occurs as large masses that grade into ferrogranophyre, as transgressive bodies as much as 10 m thick that cut ferrogranophyre, and as small veins. The granophyre is light gray or brownish gray, and the grain size is typically less than 0.1 mm. Texture is micrographic (granophyric) to aplitic. In addition to quartz and alkali-feldspar, the granophyre typically contains about 10 percent sodic plagioclase, 0.3 percent each of ferrohedenbergite and olivine or its alteration products, and less than 0.5 percent opaque minerals. Most of the olivine is completely altered to clay minerals, but the high Fe/Mg ratios of these rocks suggest that it was fayalite.

MINERALOGICAL DATA

The approximate compositions of the pyroxenes were determined from optical properties using the diagram of Carmichael (1960). Analyzed pyroxenes from other chemically similar Coast Range sills have optical properties and chemical compositions that fit this diagram better than other published diagrams relating composition and optical properties. The pyroxene ranges in composition from ferroaugite to ferrohedenbergite; no calcium-poor pyroxene was noted in any of the rocks. The pyroxene becomes progressively richer in iron (higher refractive index, Ny) in the series gabbro-ferrogranophyre-granophyre (tables 1 and 2).

The trend in pyroxene composition (fig. 3) parallels that of Ca-Fe pyroxenes from the Skaergaard intrusion (Brown and Vincent, 1963) but, at least on the basis of optical properties, is slightly more calcic. The trend is considerably more calcic than that of Ca-Fe pyroxenes from the Red Hill Dolerite of Tasmania (McDougall, 1961). All these trends, however, are toward a final composition of about $Ca_{40-43}Fe_{60-57}$ on the ferrosilite-wollastonite join, a composition similar to that of synthetic ferrohedenbergite in equilibrium with quartz and fayalite at pressures of 1 and 2 kbar (Lindsley and Munoz, 1969).

Olivine compositions were determined on mineral separates using the X-ray diffraction method (d_{130}) of Yoder and Sahama (1957). The olivine in all rocks is rich in iron, as would be expected considering that it occurs in equilibrium with quartz. In gabbro the olivine is fo_{12-19} (ferrohortonolite), and in ferrogranophyre, pegmatite, and granophyre it is fo_{4-9} (fayalite). In some granophyre olivine may be richer in iron than fo_4, but it is quantitatively minor, extensively altered, and consequently difficult to separate. Olivine is richer in iron than coexisting pyroxene in all rocks (fig. 3). Olivine is variably altered to iron-rich nontronitic clay minerals

Plagioclase compositions were determined by universal stage using the albite twin law curves of Uruno (1963). In two gabbro samples plagioclase crystal cores are an_{56}; in all others they range only from an_{51} to an_{54}. Cores constitute about 70 volume percent of individual crystals and are faintly oscillatory zoned; zonal differences are generally less than an_1. The progressively zoned outer rims are sodic andesine to calcic oligoclase. Plagioclase cores are an_{45-51} in ferrogranophyre, an_{30-51} in pegmatite, and an_{2-10} in granophyre; progressively zoned rims in ferrogranophyre and pegmatite reach oligoclase. The structural state of plagioclase is intermediate in all rocks. Some plagioclase is altered to clay minerals along crystal cracks, particularly in more silicic rocks. In most rocks, however, alteration is slight.

All euhedral quartz crystals have β quartz shape; no evidence of former tridymite was seen. The

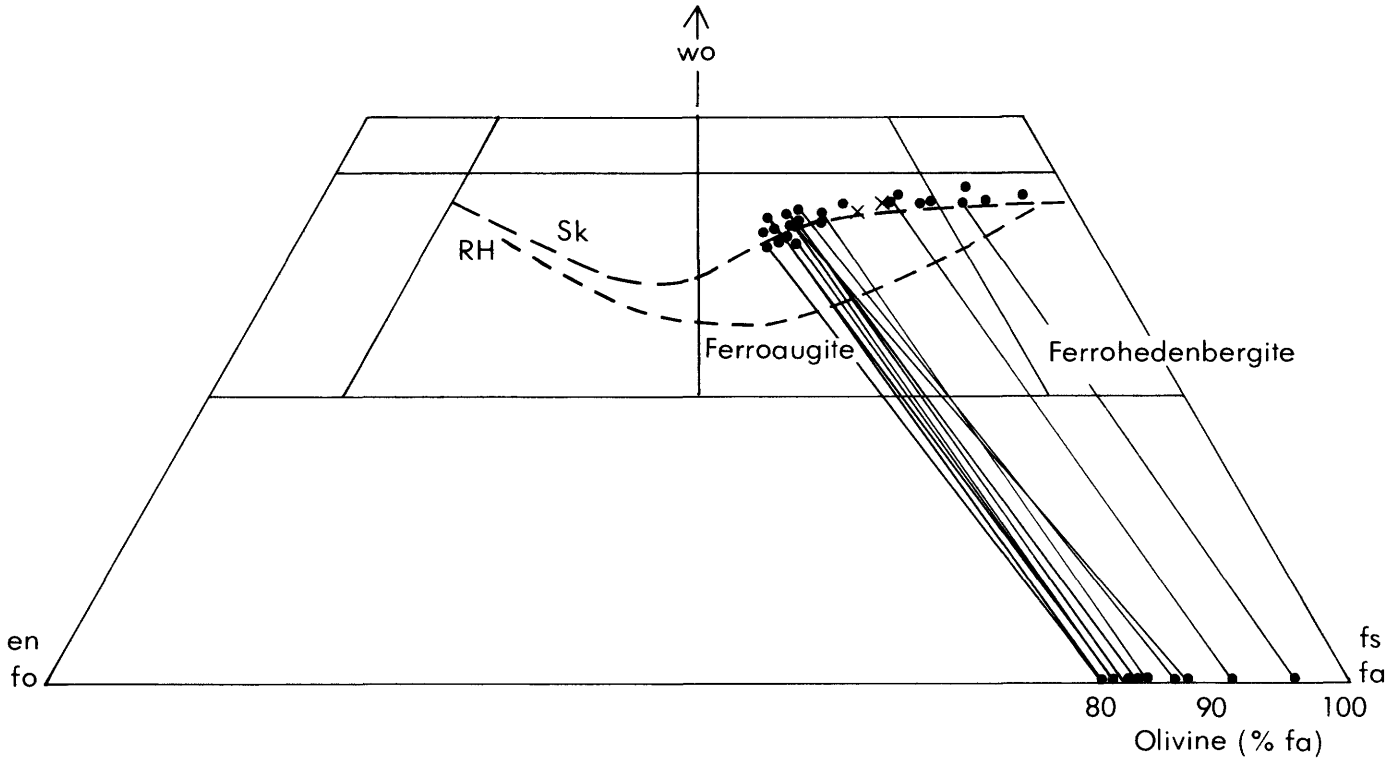

Figure 3. Inferred composition of pyroxene from Stott sill based on optical properties. Analyzed pyroxenes are labeled x; tie lines connect coexisting pyroxene and olivine pairs. wo, wollastonite; en, enstatite; fs, ferrosilite; fo, forsterite; fa, fayalite. Skaergaard (Sk) and Red Hill Dolerite (RH) pyroxene trends are shown by dashed lines.

composition of intergrown feldspar is difficult to determine optically because of its fine grain size.

TEXTURAL RELATIONS

The rocks contain subhedral to euhedral crystals of Fe-olivine, Ca-Fe pyroxene, plagioclase, opaque minerals, and apatite that are surrounded by intergrown quartz and alkali feldspar and patches of phyllosilicate minerals. The resulting granophyric and hypidiomorphic-granular texture changes from the most mafic gabbro to granophyre. In the former, the earlier minerals tend to be more commonly subhedral, and the amount of quartz-feldspar intergrowth is low (as little as 16 percent). In ferrogranophyre and granophyre, the earlier minerals tend to be more euhedral because the late-formed quartz-feldspar intergrowth is more abundant.

Cores of olivine, pyroxene, plagioclase, opaque minerals, and apatite crystals in gabbro of the lower zone are considered to be cumulus in origin. Rims on these minerals are interpreted as adcumulus growths, and the quartz-feldspar intergrowth, phyllosilicate minerals, and hornblende are intercumulus. Crystal settling is inferred to have occurred but produced neither crystal layering nor lamination, for reasons discussed later.

Ferroaugite in gabbro is equant to irregular in shape, is in places molded in subophitic fashion on smaller plagioclase laths, and projects with euhedral form into quartz-feldspar intergrowth. In some ferrogranophyre and pegmatite, the ferroaugite or ferrohedenbergite occurs as sets of parallel elongate crystals that poikilitically enclose plagioclase along their ragged borders; single crystals reach lengths of as much as 5 cm. Individual sets interlock with sets with a different orientation, producing a randomly ordered mosaic. Olivine with the same habit also occurs in these same rocks. This texture may be the result of nucleation at points within sets of interconnected Fe-Si polymers in the magma.

Olivine crystals are subhedral or anhedral where they are in contact with plagioclase and subhedral to euhedral against pyroxene; some olivine occurs as small crystals enclosed in pyroxene. Although they clearly overlap in their period of crystallization, plagioclase occurs as small crystals within olivine whereas the reverse relation is rarely seen; where observed it may result from two-dimensional view in thin section. Olivine is euhedral where bordered by quartz-feldspar intergrowth and, because of its iron-rich composition, has no reaction relation with

quartz.

The opaque minerals, about 90 percent of which are ilmenite and the remainder pyrrhotite, are typically much smaller (commonly 0.1–0.2 mm) than the other minerals except apatite. They occur enclosed in all other minerals except apatite and are particularly abundant within olivine and pyroxene crystals. The opaque minerals contain inclusions only of apatite. Most of the ilmenite appears homogeneous in polished section; only rarely are exsolution lamellae developed. Pyrrhotite occurs as small irregular masses within ilmenite and as small isolated grains.

Apatite occurs principally as 0.05 by 0.4 mm euhedra, but some very small, highly elongate crystals are also found within quartz-feldspar intergrowth. The larger apatite crystals occur within all other minerals and appear to be the first phase to begin crystallization; smaller crystals in intergrowth crystallized late.

Quartz-feldspar intergrowth and phyllosilicate patches fill in between crystals of plagioclase, pyroxene, olivine, opaque minerals, and apatite. The quartz-feldspar intergrowth consists of wavy parallel quartz rods with cuneiform cross sections that are enclosed in alkali-feldspar. Viewed parallel to quartz rods, some intergrowth appears myrmekitic; viewed perpendicular to the rods, it is micrographic. In gabbro the quartz rods are typically 0.01–0.02 mm wide and 0.2–0.3 mm long; in ferrogranophyre and pegmatite they reach 0.2–0.3 by 0.8–1 mm. Quartz and alkali-feldspar make up approximately equal proportions, but the intergrowth is so fine that it is difficult to measure their relative proportions.

The intergrowth is generally finer grained where bordered by plagioclase, pyroxene, and olivine than it is near centers of intergrowth. Near centers, quartz, and less commonly feldspar, occurs as subhedral to euhedral crystals in optical continuity with some of the surrounding intergrowth and is euhedral where it extends into phyllosilicate patches. Boundaries of intergrowth with plagioclase, pyroxene, and olivine are sharp, and no replacement of earlier minerals is indicated.

The phyllosilicate patches consist predominantly of clay minerals (probably iron-rich nontronite) with some chlorite(?) and iron-rich biotite. Ilmenite, pyrrhotite, and hornblende occur within some patches. The iron-rich clay minerals are not stable at magmatic temperatures (Ernst, 1966) so the patches were probably originally iron-rich glass that devitrified to clay minerals as the rocks cooled. This glass may have been immiscible with the residual liquid that formed the quartz-feldspar intergrowth, but if so, later crystallization has obscured any textural indications of immiscibility. However, immiscibility has been demonstrated for liquids with bulk compositions similar to those of the Stott Mountain phyllosilicates plus quartz-feldspar intergrowth (Roedder, 1951; McBirney and Nakamura, 1974; McBirney, 1975; and Irvine, 1975). Also, a 3-m-wide basalt dike south of Stott Mountain that is compositionally similar to the gabbro in the sill, and probably related to it, contains an iron-rich glass (chlorophaeite) and silicic glass in the residuum that do show textural relations of immiscibility similar to those reported by De (1974).

Iron-rich hornblende occurs principally as a marginal replacement product of pyroxene, probably as a result of reaction of pyroxenes with the residual fluids that ultimately formed the phyllosilicate patches.

ORDER OF CRYSTALLIZATION

The order of crystallization of the minerals in gabbro is inferred from textural relations. During much of the crystallization, plagioclase, olivine, ferroaugite, opaque minerals, and apatite formed together. However, of inclusion-bearing crystals, most larger plagioclase crystals contain only apatite and opaque minerals in their cores; olivine crystals contain small crystals of plagioclase, apatite, and opaque minerals; and pyroxene crystals contain small crystals of plagioclase, olivine, opaque minerals, and apatite. Opaque minerals contain apatite; crystals of apatite do not contain inclusions. Quartz-feldspar intergrowth and phyllosilicate patches fill volumes between the other minerals. These relations indicate that the order of first crystallization of the individual minerals in each rock was apatite, then opaque minerals, plagioclase, olivine, and pyroxene. Quartz-feldspar intergrowth and the phyllosilicate patches formed later.

Determining the order of first crystallization of apatite on the basis of texture may be misleading owing to its ubiquitous occurrence as euhedra in most rocks, including those from the Stott sill. However, apatite crystals that are only partially enclosed in other early-formed minerals commonly are larger where they protrude. Also, the high P_2O_5 content of the rocks (typically 0.7 percent) is consistent with apatite as an early liquidus phase.

PETROCHEMISTRY

COMPOSITION OF THE CHILLED BORDER

Four analyses of chilled border rocks all have nearly the same chemical composition (table 3) except that differing amounts of alteration of

TABLE 3.—*Chemical analyses of chilled gabbro*

[Chemical analyses were made by S. Botts, H. Smith, G. Chloe, L. Artis, J. Kelsey, J. Glenn, P. Elmore, and I. Barlow using methods described in U.S. Geological Survey Bulletin 1144A, supplemented by atomic absorption.]

Chemical analyses recalculated H_2O-free to 100 percent					
Column number---	1	2	3	4	Average of columns 1-4
Rock number-----	S68	S84	M202	M220	
SiO_2 ----------	57.1	57.2	57.2	57.9	57.4
Al_2O_3 ----------	13.3	13.4	13.3	13.4	13.4
Fe_2O_3 ----------	3.1	4.2	2.1	2.3	2.9
FeO ----------	12.3	10.7	13.4	12.4	12.2
MgO ----------	1.5	1.2.	1.4	1.7	1.5
CaO ----------	4.8	5.2	5.2	4.8	5.0
Na_2O ----------	4.9	3.2	2.9	4.2	3.8
K_2O ----------	.41	1.9	2.1	.83	1.3
TiO_2 ----------	1.7	1.9	1.7	1.7	1.7
P_2O_5 ----------	.71	.72	.67	.70	.70
MnO ----------	.23	.31	.24	.28	.27
Chemical analyses (original)					
SiO_2 ----------	54.8	55.4	55.5	55.7	
Al_2O_3 ----------	12.8	13.0	12.9	12.9	
Fe_2O_3 ----------	3.0	4.1	2.0	2.2	
FeO ----------	11.8	10.4	13.0	11.9	
MgO ----------	1.4	1.2	1.4	1.6	
CaO ----------	4.6	5.0	5.0	4.6	
Na_2O ----------	4.7	3.1	2.8	4.0	
K_2O ----------	.39	1.8	2.0	.80	
H_2O- ----------	.75	.38	.72	1.4	
H_2O+ ----------	2.7	2.0	1.8	2.2	
TiO_2 ----------	1.6	1.8	1.6	1.6	
P_2O_5 ----------	.68	.70	.65	.67	
MnO ----------	.22	.30	.23	.27	
CO_2 ----------	.05	.28	.05	.05	

feldspar and former glass(?) produce variation in the CaO, Na_2O, and K_2O content. The analyzed chilled samples are from sites as much as 8 km apart, and one is from a 7-m-thick, very fine grained sill below the main sill. The magma was apparently uniform in composition over a large area. The chilled rocks are unusual in that they have a very high total iron oxide, TiO_2, and P_2O_5 content considering their relatively silicic nature.

COMPOSITION OF ROCKS FROM THE INTERIOR OF THE SILL

The rocks in the sill show a large variation in chemical composition (tables 1 and 2). SiO_2 ranges from 51.7 to 76.1 percent, and total iron oxide from 1.6 to 18.4 percent. The combination of low MgO content (maximum 2.3 percent) and relatively high iron oxide content in all of the rocks produces an unusually high mafic index ($100x(FeO+Fe_2O_3)/(FeO+Fe_2O_3+MgO)$) that ranges from 88 to 98. Compared to the chilled margins, the least silicic rocks are enriched in total iron oxide, MgO, CaO, TiO_2 and P_2O_5 and depleted in Na_2O and K_2O. In contrast, the granophyres are enriched in alkalies and silica, depleted in other major oxides, and have a granitic composition.

The norms were determined on water-free analyses after recalculating the variable $Fe_2O_3/(FeO+Fe_2O_3)$ to 1/10 which approximates that of the least oxidized rock. A low initial oxidation state is indicated by an absence of magnetite in these iron-rich rocks; the increase in the Fe_2O_3/FeO ratio resulted from deuteric alteration. All rocks in the sill are quartz-normative. Modal quartz is greater than normative quartz (even when calculated as volume percent) because some of the normative hypersthene is represented in the rock by olivine and quartz. The normative pyroxenes plot in the iron-rich side of the pyroxene quadrilateral (fig. 3) in the "forbidden zone." Under moderately low pressure, liquids of this composition crystallize to Ca-Fe clinopyroxene, fayalitic olivine, and quartz; calcium-poor pyroxene is not stable (Smith, 1971).

COMPOSITIONAL VARIATIONS WITH HEIGHT

The modal, mineralogical, and chemical data indicate that the lower gabbro zone has a cryptic vertical variation in composition. For instance, the proportions of minerals in the zone vary systematically upward from the base to the center of the sill (fig. 4*A–D*). Olivine, opaque minerals, apatite, and plagioclase increase in abundance upward, quartz and alkali feldspar decrease, and ferroaugite, phyllosilicates, and hornblende are nearly constant (fig. 4*A*). Olivine, opaque minerals, apatite, and plagioclase are most abundant near the center of the sill.

Mineral compositions also change vertically (fig. 4*B*). Ferroaugite shows a slight progressive increase in Mg/Fe ratio (shown by slight decrease in Ny) from the base to a maximum near the center even though the amount of ferroaugite does not change significantly. Olivine is also progressively richer in magnesium, ranging from fo_{12-13} near the base to fo_{19} near the center. Plagioclase crystals are zoned, so it is difficult to determine their vertical variation in bulk composition. However, crystal cores in the lowest two samples are an_{51}, whereas near the center of the sill most are an_{54}. This apparent upward increase in core anorthite content is paralleled by an upward increase in normative an/an+ab from 42–43 near the base to 46–50 near the sill center.

The chemical composition of the rocks also changes vertically (fig. 4*C–D*). From the base to the center of the sill, total iron oxide , MgO, CaO, TiO_2, and P_2O_5 increase; Al_2O_3 remains nearly constant;

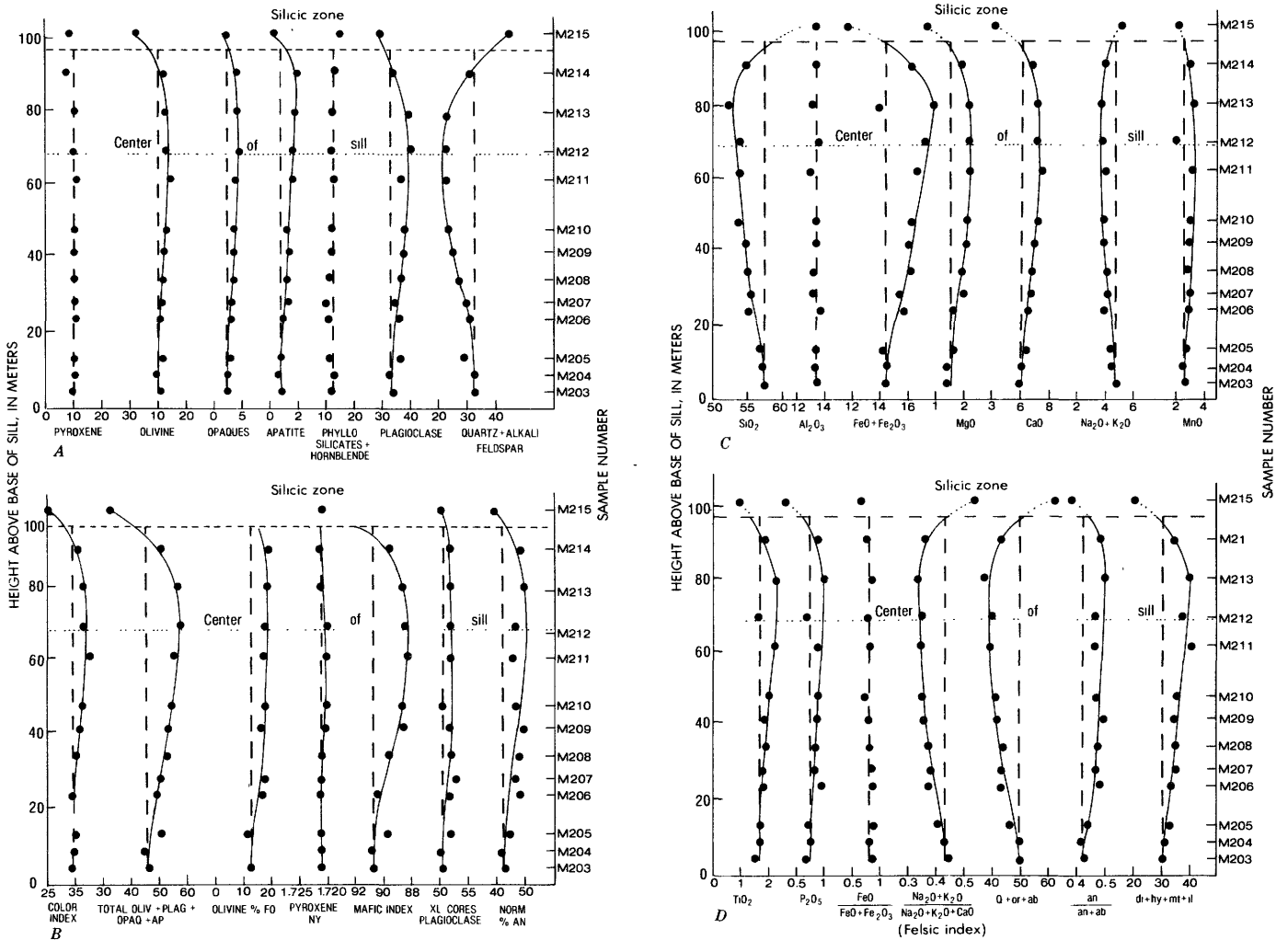

Figure 4. Vertical variation in lower gabbro zone. *A*, Modes. *B*, Mineral compositions and chemical data. *C*, Major oxides. *D*, Oxide ratios.

and SiO_2, Na_2O, and K_2O decrease. The differentiation index (Q+or+ab), mafic index, and felsic index decrease systematically from the base to the center of the sill (fig. 4*B–D*). The differentiation index parallels the change in amounts of quartz and alkali feldspar, the mafic index in part reflects the change in Mg/Fe of ferroaugite and olivine, and the change in felsic index correlates with plagioclase composition and amount of alkali feldspar.

The modal, mineral, and chemical data indicate that composition changes systematically from the base to above the center of the sill and that the center is most mafic (femic). Most other differentiated dolerite or gabbro sills are most mafic at a much lower position, usually nearer the base than the center.

Most rocks in the silicic zone in the area where the rocks of table 1 and figure 4 were collected are weathered and only four were suitable for analysis (table 2, cols. 5, 6, 7, and 10); three are silicic gabbro and one is ferrogranophyre. The weathered rocks there and elsewhere are mostly ferrogranophyre. The remaining analyses of ferrogranophyre, pegmatite, and granophyre shown in table 2 are from the silicic zone at other locations at and near Stott Mountain. They show that rocks in the silicic zone contain more SiO_2, and K_2O and less total iron oxide, MgO, CaO, TiO_2, and P_2O_5 than does the rest of the sill. Elements that are enriched in the silicic zone are those that are impoverished in the lower gabbro zone compared to the chilled margins.

BULK COMPOSITION OF THE SILL

The bulk composition of a differentiated sill must approximate the original chilled margin composition if chemical variation resulted from closed-system differentiation of magma in place. As with many

TABLE 4.—*Average compositions of rocks*

Column number----	1	2	3	4	5	6
	Lower gabbro zone[1]	Silicic zone[2]	Upper gabbro zone[2]	Chilled gabbros[3]	Lowest three gabbros[4]	Bulk composition[5]
SiO_2 ----------	54.7	64.6	56.5	57.4	57.3	57.3
Al_2O_3 ----------	13.3	13.6	13.5	13.4	13.4	13.4
$FeO + 0.9\ Fe_2O_3$ -	16.0	9.6	14.9	14.8	14.2	14.4
MgO ----------	1.9	0.67	1.5	1.5	1.5	1.6
CaO ----------	6.9	3.9	6.0	5.0	6.3	6.1
Na_2O ----------	2.7	3.7	2.8	3.8	2.9	2.9
K_2O ----------	1.4	2.5	1.6	1.3	1.7	1.7
TiO_2 ----------	1.9	1.0	1.9	1.7	1.6	1.7
P_2O_5 ----------	.83	.33	.70	.70	.71	.70
MnO ----------	.29	.17	.25	.27	.27	.26

[1]Average of analyses in table 1 weighted according to interval thickness represented by each analysis.

[2]Average of all analyzed rocks in zone.

[3]Average of four chilled gabbro analyses listed in table 3.

[4]Average of rocks 203-205, table 1.

[5]Weighted average of three zones according to interval thickness represented by each zone.

gabbro and dolerite sills, however, the original composition of the chilled margins of this sill has been modified slightly by deuteric alteration and weathering. Alteration has caused variations in alkalies and CaO but little change in the other major oxides. Alteration effects are best seen by comparing analyses of the chilled margin rocks to those of little-altered rocks from close to the chilled margins (table 4, cols. 4 and 5).

The bulk composition of the sill can be calculated from compositions and thicknesses of the three zones that make up the sill. The composition of the lower gabbro zone, which forms 70 percent of the sill, can be determined accurately because rocks within the zone show a systematic vertical variation in composition defined by 12 analyzed rocks. The bulk composition of this zone (table 4, col. 1) was obtained by adding the compositions of the individual intervals weighted according to the interval thickness.

The composition of the silicic zone, which forms about 25 percent of the sill, is not so readily obtained because of its heterogeneity. The average composition of all analyzed rocks from the silicic zone is assumed to be approximately equal to the bulk composition of this zone. This average composition (table 4, col. 2) is similar to an analyzed ferrogranophyre (table 2, col. 10) that is typical of the most abundant rock in the silicic zone.

The bulk composition of the sill (table 4, col. 6) was determined by adding appropriate proportions of the average composition of each zone. For instance, 70 percent of the average SiO_2 of the lower zone plus 25 percent of the average SiO_2 of the silicic zone and 5 percent of the SiO_2 of the upper gabbro zone equals the bulk SiO_2 composition of 57.3 percent SiO_2.

The average chilled margin composition (table 4, col. 4) is virtually identical to the calculated bulk composition. This result indicates that the variations

TABLE 5.—*Compositions of successive residual liquids*

[Residual liquid compositions were determined using bulk composition of sill (table 4, col. 6) equal to composition of sill at time of emplacement (0 percent solidified) and successively subtracting compositions or rocks starting at the base of the sill and progressing inward with each rock analysis weighted according to interval thickness it represents. For purposes of the calculation the average gabbro analysis from the upper gabbro zone was used for all rocks in that zone. The average composition of all rocks in the silicic zone is presumed to approximately equal the composition of the residual liquid when the silicic zone first began to form (75 percent solidified) and the average granophyre to approximately equal the liquid at 95-100 percent solidified.]

Percent solidified-	0	20	25	30	35	43	50	59	67	75	95-100
SiO_2	57.3	57.4	57.5	57.7	58.0	58.5	59.4	60.3	62.3	64.6	74.5
Al_2O_3	13.4	13.4	13.4	13.4	13.4	13.4	13.5	13.5	13.6	13.6	13.2
FeO + Fe_2O_3	14.4	14.3	14.2	14.1	13.9	13.6	13.1	12.4	11.1	9.6	2.8
MgO	1.6	1.6	1.6	1.6	1.5	1.4	1.3	1.2	.94	.67	.14
CaO	6.1	6.1	6.0	6.0	5.9	5.7	5.4	5.1	4.6	3.9	.54
Na_2O	3.0	3.0	3.0	3.0	3.1	3.1	3.2	3.3	3.4	3.7	4.6
K_2O	1.7	1.7	1.7	1.7	1.7	1.8	1.9	2.0	2.2	2.5	3.6
TiO_2	1.7	1.7	1.6	1.6	1.6	1.5	1.5	1.4	1.2	1.0	.32
P_2O_5	.70	.69	.67	.66	.65	.62	.58	.56	.45	.33	.02
MnO	.26	.25	.25	.25	.24	.23	.22	.22	.20	.17	.07
NORMS (Calculated with Fe_2O_3 = 10 percent total iron)											
Q	12.3	12.4	12.6	12.9	13.1	13.7	14.5	15.5	17.9	19.7	30.8
or	10.1	10.1	10.1	10.1	10.1	10.6	11.2	11.8	13.0	14.8	21.3
ab	25.4	25.4	25.4	25.4	26.2	26.2	27.1	27.9	28.8	31.3	38.9
an	18.1	18.1	18.1	18.1	17.6	17.3	16.9	16.1	15.4	13.1	2.6
di: wo	3.2	3.2	3.1	3.1	3.1	2.9	2.6	2.3	1.9	1.7	-
di: en	.6	.6	.6	.6	.5	.5	.4	.4	.3	.2	-
di: fs	2.9	2.9	2.8	2.8	2.8	2.7	2.4	2.2	1.8	1.7	-
hy: en	3.4	3.4	3.4	3.4	3.2	3.0	2.8	2.6	2.1	1.5	.4
hy: fs	17.4	17.2	17.3	17.2	16.8	16.7	16.1	15.4	14.0	12.1	4.0
mt	2.1	2.1	2.1	2.0	2.0	2.0	1.9	1.8	1.6	1.4	.4
il	3.2	3.2	3.0	3.0	3.0	2.9	2.9	2.7	2.3	1.9	.6
ap	1.7	1.6	1.6	1.6	1.5	1.5	1.4	1.3	1.1	.8	-

in composition of the sill resulted from differentiation of magma in place. Had there been multiple injection of magma (for which there is no evidence), then either the magmas were similar in composition or the amount of later magma of different composition was small. Furthermore, no significant amount of sedimentary rocks could have been assimilated after the chilled margins formed.

RESIDUAL LIQUID COMPOSITIONS

Residual liquid compositions were determined by subtracting the compositions of successive intervals of rock starting at the margins of the sill and progressing toward the interior. The bulk residual liquids can be calculated only for the interval during which the lower and upper gabbro zones solidified because these show systematic changes in rock compositions whereas the order of formation of rocks within the silicic zone is poorly known. Compositions of the residual liquids are shown in table 5. Although the calculated residual liquid compositions define the gross changes in the bulk magma during solidification, they do not necessarily represent the liquid compositions near the sites of crystallization because of crystal growth and settling and because the liquid in the sill could not have been perfectly homogenized. Furthermore, the residual liquid compositions that were calculated are those of the

TABLE 6.—*Comparison of calculated residual liquids to compositions of mixtures of analyzed rocks and silicic liquids*

Height (meters) ------	13-1/2		24-1/2		29		35		42-1/2	
Percent solidified ---	10		19		22		27		32-1/2	
Factor[1] ----------	0.062		0.278		0.287		0.371		0.467	
	205 Liq.[2]	205 Calc.[3]	206 Liq.	206 Calc.	207 Liq.	207 Calc.	208 Liq.	208 Calc.	209 Liq.	209 Calc.
SiO_2 ----------	57.3	57.3	57.4	57.4	57.5	57.5	57.6	57.6	57.9	57.9
Al_2O_3 ----------	13.4	13.4	13.4	13.7	13.4	13.3	13.4	13.3	13.4	13.5
$FeO + Fe_2O_3$ ----------	14.4	14.1	14.3	14.4	14.3	14.2	14.2	14.3	14.0	14.0
MgO ----------	1.6	1.6	1.6	1.4	1.6	1.7	1.6	1.6	1.6	1.7
CaO ----------	6.1	6.4	6.1	5.9	6.1	6.2	6.0	6.0	6.0	6.0
Na_2O ----------	3.0	2.8	3.0	2.9	3.0	2.9	3.0	2.9	3.0	2.9
K_2O ----------	1.7	1.8	1.7	1.6	1.7	1.7	1.7	1.8	1.7	1.8
TiO_2 ----------	1.7	1.7	1.7	1.6	1.7	1.6	1.6	1.7	1.6	1.6
P_2O_5 ----------	.70	.71	.69	.80	.68	.73	.67	.69	.66	.70
MnO ----------	.26	.27	.25	.26	.25	.27	.25	.26	.25	.27
Height (meters) ------	49		62-1/2		70		81		91	
Percent solidified ---	37-1/2		48		53		62		70	
Factor ----------	0.693		1.018		1.264		2.600		5.670	
	210 Liq.	210 Calc.	211 Liq.	211 Calc.	212 Liq.	212 Calc.	213 Liq.	213 Calc.	214 Liq.	214 Calc.
SiO_2 ----------	58.2	58.2	59.1	59.1	59.7	59.7	61.1	61.1	63.1	63.1
Al_2O_3 ----------	13.4	13.5	13.5	13.3	13.5	13.6	13.5	13.5	13.6	13.6
$FeO + Fe_2O_3$ ----------	13.8	13.6	13.3	13.1	13.5	13.6	13.5	13.5	13.6	13.6
MgO ----------	1.5	1.5	1.3	1.4	1.3	1.4	1.1	1.1	.85	.85
CaO ----------	5.8	5.9	5.5	5.7	5.3	5.4	4.9	4.8	4.4	4.4
Na_2O ----------	3.1	3.1	3.2	3.2	3.2	3.3	3.4	3.4	3.5	3.5
K_2O ----------	1.7	1.8	1.9	1.9	1.9	1.8	2.1	2.1	2.3	2.3
TiO_2 ----------	1.6	1.6	1.5	1.5	1.5	1.3	1.3	1.4	1.1	1.1
P_2O_5 ----------	.64	.65	.60	.60	.57	.49	.51	.52	.41	.41
MnO ----------	.24	.25	.22	.24	.22	.18	.21	.21	.19	.19

[1]Factor is the amount of liquid with composition of the silicic zone (SiO_2=64.6) added to each rock to match the SiO_2 of the calculated mixture with the residual liquid composition.

[2]Interpolated values from table 5.

[3]SiO_2 of residual liquid and calculated mixture are by definition the same, all other oxides of the mixture are calculated using the factor determined to balance the SiO_2 contents.

bulk liquid plus all crystals suspended in it.

The residual liquid compositions can be closely duplicated by combining each analyzed rock and an appropriate proportion of liquid more silicic than the calculated residual liquid. In table 6, the residual liquid compositions are compared to calculated mixtures of each rock and an appropriate amount of liquid whose composition is that of the average silicic zone rock (table 4, col. 2). The calculations were made so as to duplicate the SiO_2 content of the residual liquid (as for example, for rock 211, SiO_2 of rock = 53.5, SiO_2 of residual liquid at the time of formation of rock

211 = 59.1, as extrapolated from table 5, SiO_2 of silicic zone = 64.6, thus

$$\frac{1(53.5) + x(64.6)}{1+x} = 59.1, \text{ and } x = 1.018.$$

All other oxides of the mixture were calculated using 1 part of rock 211 and 1.018 parts of composition like that of the silicic zone rock). Similar results can be obtained using liquids more or less silicic than the average silicic zone rock. The similarity of the mixtures to the residual liquid compositions indicates that removal of relatively silicic liquid residues from crystal accumulations can produce the observed rock compositions.

CHEMICAL VARIATION

The composition of the analyzed rocks and calculated successive bulk residual liquids are plotted on a solidification diagram (Wager, 1960) in figure 5. It shows the composition of the rocks that formed at various stages during the solidification of the magma and the corresponding gross changes in the magma's bulk composition.

The successive residual liquids began to differ appreciably from the initial composition when the sill was about 20 percent solidified. With respect to the initial bulk composition, the liquid was enriched in SiO_2, Na_2O, and K_2O and depleted in all other major oxides except Al_2O_3, which remained nearly constant. The liquid progressively changed composition until the last liquid crystallized and, at this end stage, differed greatly in composition from the initial liquid. The liquid trends are smoother than the rock trends because the former were determined using successive rock analyses, which tend to smooth out the small scatter shown by the rock analyses. Much of the scatter in this and succeeding diagrams is within the range of analytical error for rapid-rock analyses. The CaO content of the rocks reached its maximum when the sill was 50 percent solidified, and $FeO+Fe_2O_3$, MgO, TiO_2, and P_2O_5 were maximum when the sill was about 60 percent solidified. This stage in the solidification corresponds to the formation of the upper part of the lower gabbro zone and approximately to the crystallization of rock M213. The rock composition trends for all oxides cross the bulk composition lines at a time corresponding to 75 percent solidification. Thus rocks that formed at about this stage (for example, table 2, col. 6) may have compositions similar to the bulk composition and the chilled margins, although much different from the residual liquid from which they crystallized.

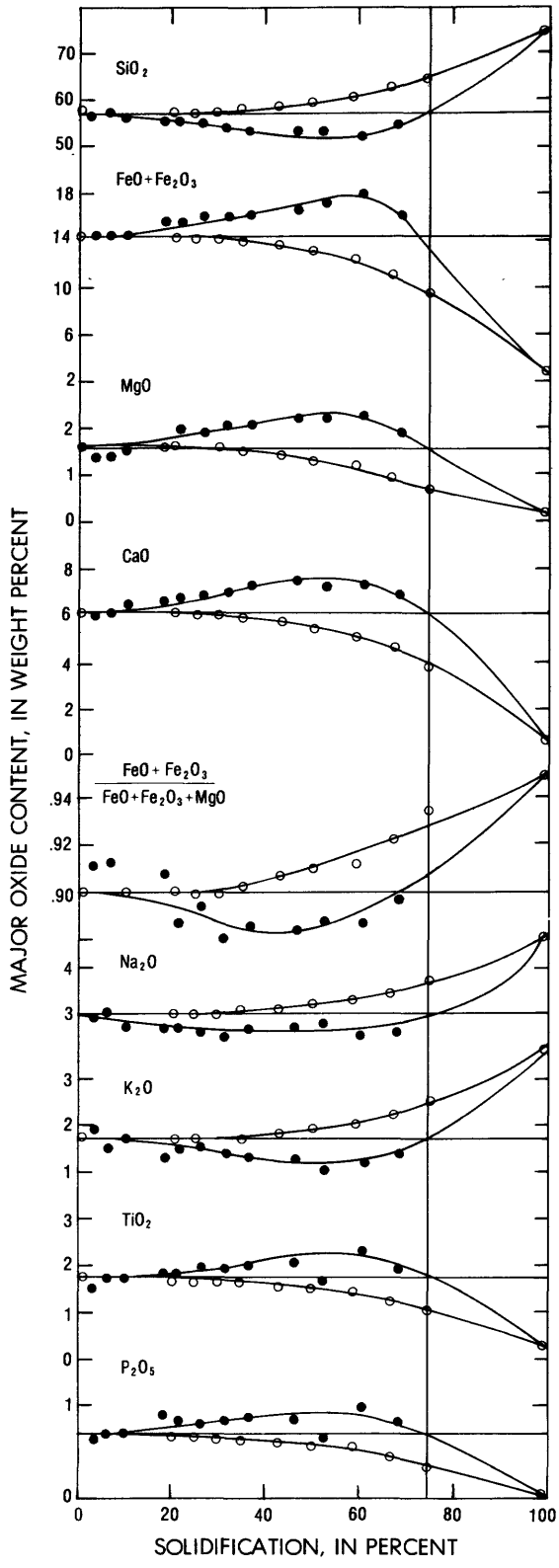

Figure 5. Solidification diagram showing amount of major oxides in rocks and bulk residual liquids at various stages in solidification of gabbro sill. Rock trends are shown by a solid circle and liquid trends by an open circle. Horizontal lines show bulk composition of sill; vertical line at 75 percent solidification indicates beginning of formation of silicic zone.

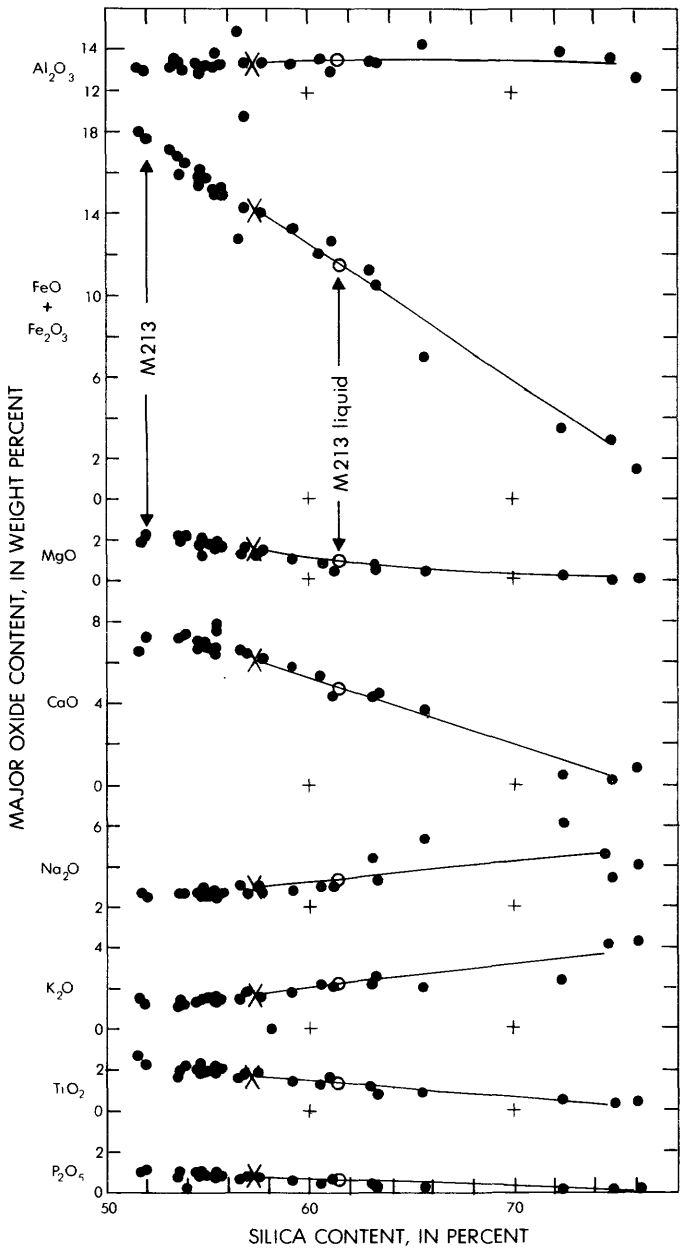

Figure 6. Silica variation for rocks from gabbro sill. Bulk composition shown by x, residual liquid compositions are shown by solid lines, and composition of residual liquid at time of crystallization of gabbro M213 is shown by open circle.

The rocks show a concomitant increase in Na_2O and K_2O, relatively constant Al_2O_3, and decrease in total iron, MgO, CaO, TiO_2, and P_2O_5 with respect to increase in silica (fig. 6). The rock analyses plot along smooth curves except for those with high SiO_2 content, which show some scatter, especially with respect to Na_2O and K_2O (total alkalies, however, plot along a smooth curve). As the sill solidified, the newly formed rocks had a progressively lower silica content starting at 57 percent SiO_2 (chilled margin and bulk composition) and decreasing to 52 percent

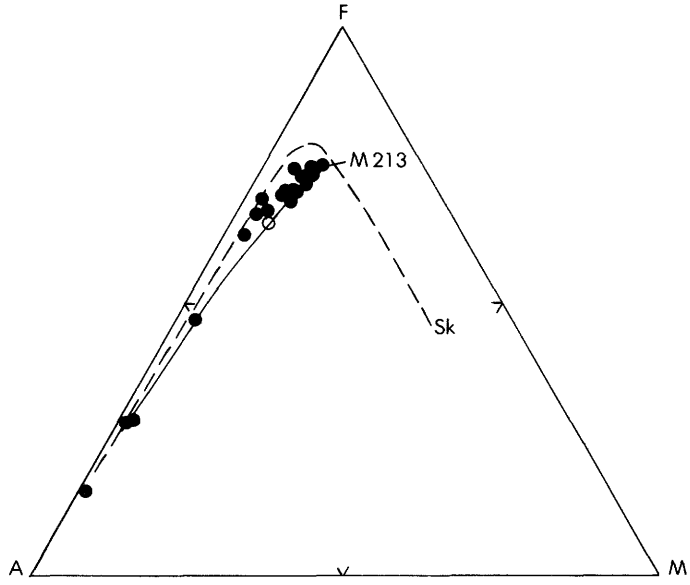

Figure 7. FMA (F=FeO+0.9Fe_2O_3+MnO, M=MgO, A=N_2O+K_2O) diagram of analyzed rocks and residual liquids of Stott sill. Open circle shows composition of residual liquid at time of formation of rock M213; solid line shows variation in composition of residual liquids; and dashed line Sk shows Skaergaard trend.

SiO_2 (sample M213, table 1) when the sill was about 60 percent solidified. After that, the rocks were successively enriched in SiO_2 until formation of the granophyre with 76 percent SiO_2.

The analyzed rocks all have high Fe/Mg ratios and plot along a nearly linear trend on an FMA diagram (fig. 7). Unlike many other differentiated dolerite or gabbro sills, the rocks from the Stott Mountain sill show no marked early change in the uniformly high Fe/Mg ratio. On the basis of 200 analyses of rocks from related sills in the Oregon Coast Range (P. D. Snavely, Jr., and N. S. MacLeod, unpub. data), however, this unusual F-A trend is characteristic, and none of the sills show an F-M trend. The bulk composition of the Stott sill, with its high Fe/Mg ratio, is much like that of late-stage rocks of many differentiated dolorite sills. Rock compositions changed initially to lower relative alkali content and slightly lower Fe/Mg ratios until about 40 percent residual liquid remained, at which time sample M213 crystallized, and then showed a marked relative increase in alkalies. In contrast, the residual liquid trend is toward continuously higher alkali content.

PROCESS OF DIFFERENTIATION

Any explanation of the processes of differentiation of the gabbro sill must take into account the following:

(1) The sill is thin compared to other gabbro, diabase, or dolerite sills that show similar degrees of

differentiation.

(2) Agreement between the calculated bulk composition and the chilled margin composition shows that no large amount of material could have been assimilated by the magma within the sill and that there could not have been large additions of magma of different composition. The sedimentary rocks marginal to both the Stott Mountain sill and the related Marys Peak sill also have compositions (Snavely and others, 1969) grossly different from the sill rocks (that is, the sedimentary rocks have more MgO and Al_2O_3). Also, no field evidence was found for assimilation of sedimentary country rock or multiple intrusion. Furthermore, lead-isotope ratios of gabbro, granophyric diorite, pegmatite, and granophyre from the Marys Peak sill are uniform and differ from isotope ratios of the sedimentary rocks intruded by the sill (Tatsumoto and Snavely, 1969).

(3) Neither rhythmic layers nor crystal lamination were observed. The gabbro is uniformly homogeneous in gross aspect even though the lower half of the sill shows vertical chemical and mineralogic variations.

(4) Differentiation of the magma produced asymmetric trends in rock compositions, mineral proportions, and mineral compositions. Rocks show a progressive increase in MgO, total iron oxide, CaO, TiO_2, and P_2O_5, and decrease in SiO_2 and alkalies, from the base toward the center of the sill. Plagioclase, olivine, opaque minerals, and apatite increase in abundance, and pyroxene and olivine are progressively richer in magnesium over the same interval. The most mafic rock occurs somewhat above the center of the sill, and silicic rocks occur at a high level.

(5) The sill was intruded under a thick cover of sedimentary rocks in middle Oligocene time. Much of the cover has been eroded, but farther west, Eocene and lower Oligocene marine sandstone and siltstone have a thickness of about 1.5 km (Snavely and others, 1976), and the sill was intruded near the base of this sequence. Owing to the insulating cover, conductive heat loss should have been about the same from the base and top of the sill during solidification (Jaeger, 1957, p. 312), unless convection, crystal settling, or some other process of heat transport was involved. Convection and crystal settling both cause asymmetric heat loss resulting in final solidification in the upper part of a sill rather than at its center (Irvine, 1970).

(6) The chilled margins are aphyric, and the magma was therefore near or above liquidus temperature.

(7) The last minerals to crystallize in early-formed rocks have bulk compositions grossly similar to the composition of late-formed rocks.

(8) The parent magma had an unusual composition (that is, high SiO_2, P_2O_5, and total iron, and low MgO).

A differentiation process that appears to account for the distribution of rock types, the mineralogic and chemical variations, and absence of rhythmic layers and crystal lamination combines the progressive inward crystallization proposed by Hess (1960) with crystal settling within zones of crystallization at the floor and roof of the liquid interior of the sill. Differentiation as a result of crystal settling within crystallization zones has been discussed by Jackson (1961), Wilshire (1967), and Irvine (1970). Richter and Moore (1966) report such a transient downward-moving zone of crystallization beneath the developing crust of the Kilauea lava lake.

According to the suggested model, as the sill solidified, one crystallization zone moved continuously upward from the base and another downward from the top (fig. 8). Inferred relations in the lower zone of crystallization are shown in figure 9. The order of nucleation of the minerals shown by textural relations suggests that the minerals first nucleated at different heights within the zone. Thus, the top of the lower zone contained magma plus apatite crystallites, the first mineral phase to nucleate. Progressively lower parts contained (1) magma, apatite, plus opaque minerals; (2) magma, apatite, opaque minerals, plus plagioclase; (3) magma, apatite, opaque minerals, plagioclase, plus olivine; (4) magma, apatite, opaque minerals, plagioclase, olivine, plus ferroaugite; and (5) at the base of the zone, apatite, opaque minerals, plagioclase, olivine, ferroaugite, plus quartz-feldspar intergrowths. Even though the various minerals first nucleated at different heights in the zone of crystallization, in successively lower positions they continued to grow and react with residual liquid.

The early-formed minerals in the lower zone of crystallization were denser than the enclosing magma and thus would have settled. In order broadly to define relative settling velocities (fig. 10), the approximate viscosity and density of the residual bulk magmas were calculated from their chemical compositions using the methods of Shaw (1972) and Bottinga and Weill (1970), respectively. Crystals were assumed to have the same volumes as they do in the rocks but, for simplification, were assumed spherical; Jackson (1971) shows that elongate crystals will settle about 10 percent more slowly than spheres of the same volume. According to the model,

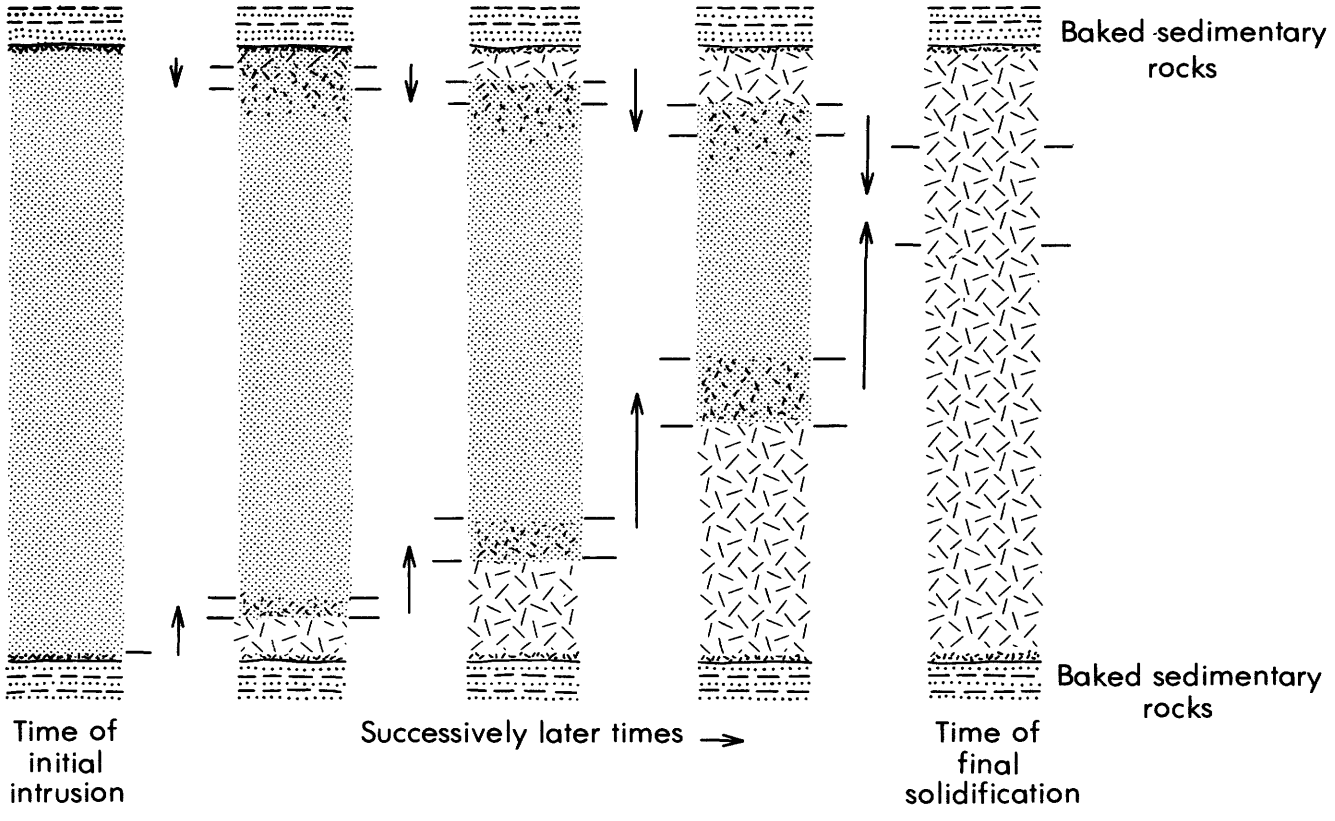

Figure 8. Progressive solidification of gabbro sill. Horizontal lines delimit upper and lower zones of crystallization; arrows indicate direction of solidification.

the crystal size would increase downward in the lower crystallization zone; if the crystals grew continuously in size during settling, their initial velocity would be much lower and average settling velocity would be only one-third that of crystals with constant size, assuming constant viscosity. Thus, the calculated rates for various temperatures and liquid compositions (fig. 10*A*, *B*) are somewhat greater than the actual rates would have been if crystals settled as individuals. Settling of crystal aggregates formed as a result of heterogeneous nucleation (Campbell, 1978), on the other hand, would be more rapid than settling of individuals.

Numerous laboratory experiments show that crystallization of basaltic magmas commonly occurs over a 100°-200°C temperature interval. No data are available for rocks with compositions similar to those in the sill, but a similar temperature interval appears reasonable; considering the unusual composition, the interval may even have been greater. The temperature interval over which the various minerals crystallized and settled would change as the lower crystallization zone migrated upward because the bulk residual magma became progressively more silicic in composition.

Crystals nucleating in the upper part of the crystallization zone would not settle until they reached a size large enough to overcome the yield strength of the magma. Upon reaching sufficient size, they would begin to settle, and the rate would increase as their size increased at progressively lower positions in the zone. At even lower positions, the rate would decrease because the remaining residual liquid at successively lower positions would have had a continuously higher viscosity (more silicic composition and lower temperature). To a certain extent, the downward decrease in settling rate caused by increasing viscosity may have been counteracted by an increasing tendency for crystals (because of higher crystal content) to settle as aggregates at a rate higher than they would as individuals.

The combined effect of changing temperature and liquid composition (arbitrarily related) on settling rate are shown diagrammatically in figure 10*C*. Without liquidus temperature determinations it is not possible to speculate on the thickness of the crystallization zone nor on the heights within the zone at which the various minerals would nucleate. Figure 10*C* does indicate, however, that the settling

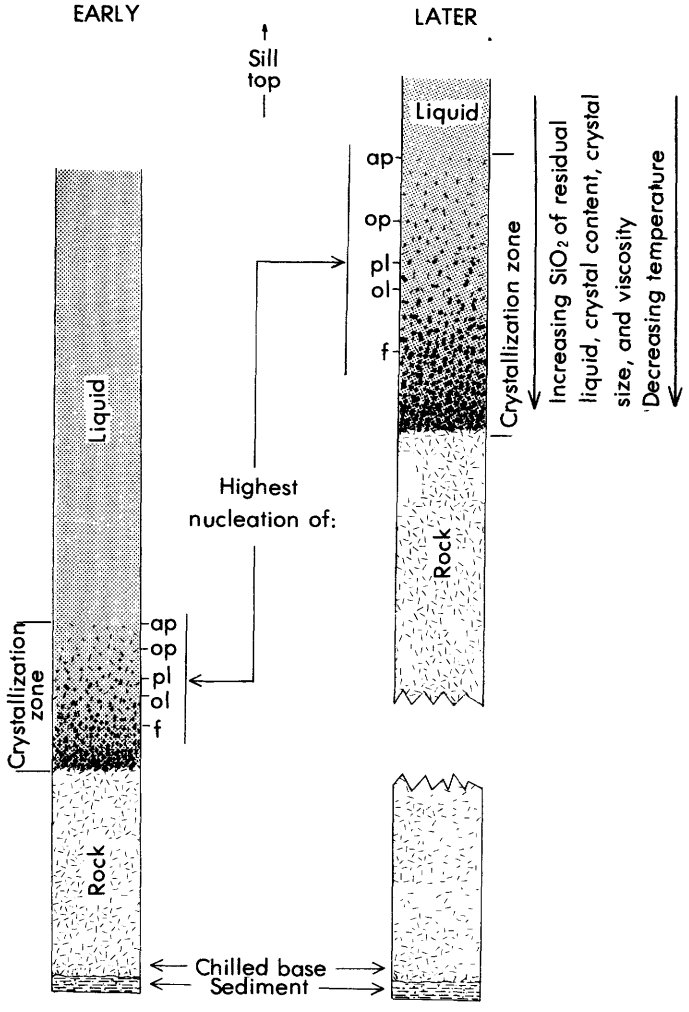

Figure 9. Inferred crystallization and settling of minerals in lower zone of crystallization at two different periods in solidification of gabbro sill. ap, apatite; op, opaque minerals; pl, plagioclase; ol, olivine; f, ferroaugite.

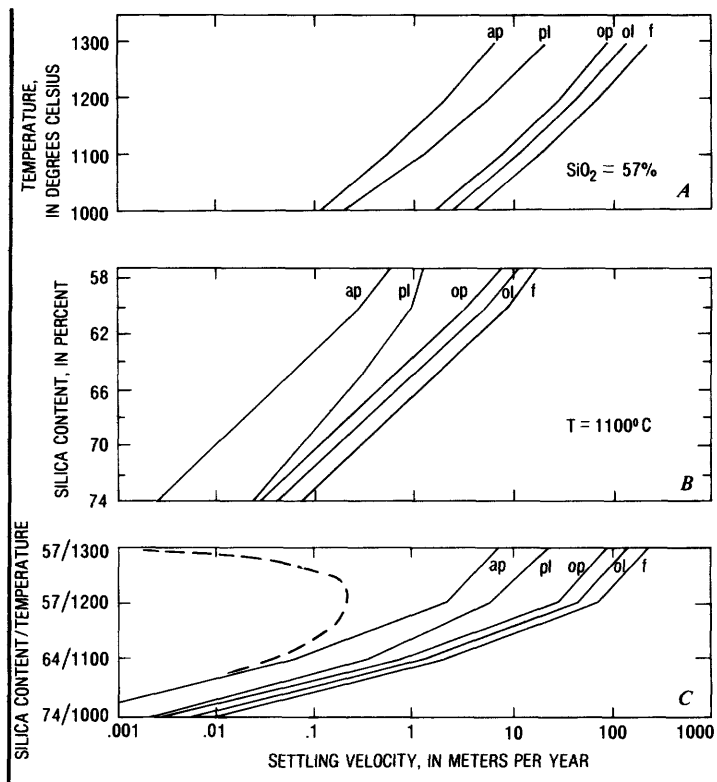

Figure 10. Calculated settling rates of apatite (ap), plagioclase (pl), opaque minerals (op), olivine (ol), and ferroaugite (f), as a function of temperature and silica content of residual liquid. *A*, Decrease in settling rate with decrease in temperature. Calculated viscosity ranges from 6.7×10^2p at 1300°C to 3.6×10^4p at 1000°C and density increases from 2.56 to 2.60 over same interval. *B*, Decrease in settling rate as a function of increasing SiO_2 content of residual liquid with viscosity of least silicic liquid of 7.8×10^3p increasing to 2.3×10^6 for most silicic and density decreasing from 2.58 to 2.33 over same range. *C*, Marked decrease in settling rate that results from decreasing temperature and increasing silica content of liquid. Settling rates were calculated based on constant crystal size; actual settling rates would have shapes shown by dashed line if crystal growth were taken into account.

rates would have decreased by an order of magnitude from the upper to the lower part of the zone even if it represented a temperature interval of only 100°C. The settling rates would have been so low near the base even for crystal aggregates that the crystals would effectively become frozen in position at a height higher than the point at which an intact crystal framework (about 50 percent crystals) would itself inhibit further settling. Thus in the absence of a well-defined floor and because of the extremely low settling velocity in the lower parts of the zone, crystal lamination could not result from crystal settling, nor would the resulting textures be obviously cumulate.

The calculated settling rates appear to be generally consistent with the model of crystallization zone settling, considering the apparent orders of nucleation of the minerals and the amount of upward increase they show in the rocks of the lower gabbro zone. Apatite, the first phase to nucleate, shows the greatest relative upward increase in amount in the lower gabbro zone. As the calculated settling velocity for apatite is very low (small crystal size), for it to have accumulated in large amount by settling requires that it settle from a very high position relative to the other minerals. Thus, for much of the zone, only apatite could have been present in the magma. Apatite crystals commonly do occur enclosed in olivine so they would have in part settled as aggregates at a higher rate, but much of the apatite must have settled as individual crystals because it increases in amount upward more than does olivine. Early crystallization of apatite is consistent with the very high P_2O_5 content of the magma (bulk composition has 0.7 percent P_2O_5).

Opaque minerals nucleated after apatite. Because

they have a much higher calculated settling rate, yet increase in abundance upward nearly as much as apatite, the height at which opaque minerals became large enough to settle must have been far below that of apatite.

Plagioclase nucleated after apatite and opaque minerals, thus at a lower position in the crystallization zone, but its calculated settling velocity is very low (low density contrast with the magma), consistent with the minor upward increase it shows. The calculated settling velocity for plagioclase is the least reliable, for its density contrast with the liquid is so low that slight differences between the actual and calculated magma density greatly affect settling rate. However, aggregate grains including plagioclase would settle at rates higher than those calculated.

Olivine nucleated next and increases upward more than plagioclase because it has a settling rate an order of magnitude greater. Ferroaugite, the last cumulus phase to nucleate, has the highest calculated settling velocity yet remains about constant in amount throughout the lower gabbro zone. Apparently at its low position of nucleation and growth in the zone, the viscosity of the remaining residual liquid was high, and ferroaugite settled much less than the other minerals. Even though ferroaugite does not significantly change in abundance upward, it nevertheless must have settled to some extent because the bulk residual magma composition was changing: the absence of ferroaugite settling would correspond to an upward decrease in ferroaugite. Compaction of the crystal mush in the lowest part of the crystallization zone may have been sufficient to increase the proportion of ferroaugite slightly compared to the amount produced by an increasingly more silicic magma with less potential ferroaugite.

Residual magma displaced upward by crystal settling within the lower zone would be depleted in components of the early-formed minerals and less dense than the magma overlying the zone of crystallization. The displaced residual magma may have diffused into the overlying magma in response to density, chemical, and thermal gradients. That part of the residual magma which remained trapped in the lower part of the zone ultimately formed adcumulus rims on crystals and the intercumulus quartz-feldspar intergrowth and phyllosilicate patches.

The phyllosilicate patches initially decrease in abundance upward and then increase toward the center of the sill to a value similar to that near the base. This increase may result from a possible immiscible relation between the iron-rich liquid from which these patches were formed and the silicic residual melt that crystallized as intergrowth. Perhaps the residual liquids within the lower crystallization zone were initially displaced before immiscibility could occur, whereas during later stages the residual liquid unmixed and only the light silicic residual liquid was displaced upward.

On the basis of the calculated magma viscosity and the thickness of the sill, it seems likely that magma within the interior of the sill would convect (Bartlett, 1969, fig. 1). No evidence indicating convection was found, but the lower crystallization may have lain quiescent below the convecting interior, such as Jackson (1961, p. 97) postulated for the Stillwater Complex of Montana. Convection in the interior of the sill would have tended to homogenize displaced residual magma with magma in the interior.

When the lower zone of crystallization was near the base of the sill, crystal settling would have been minor because the zone was thin (steep thermal gradient) and its base (surface of complete solidification) moved rapidly upward. The early crystals in the zone would have reacted with entrapped residual interstitial liquid, and the bulk composition of the rock would be virtually unchanged from that of the original magma. As a sill cools, isotherms progress inward from the contacts approximately in proportion to the square root of time (Jaeger, 1957, p. 79). Therefore, the distance between any two isotherms, such as bounded the lower zone of crystallization, would increase as they migrated upward (figs. 8 and 9). The distance from top to bottom of the zone would increase even though the bounding isotherms would change as the zone migrated upward as a result of changing residual magma composition. Consequently, because increasing time would be available as the crystallization zone moved upward, the efficacy of crystal settling would increase and progressively more residual liquid would be displaced.

Such a process is suggested by the data of table 6 in which residual liquid compositions are closely approximated by mixtures of analyzed rocks and relatively silicic liquids. The proportion of displaced silicic liquid (factor of table 6) increases with the degree of solidification and height (fig. 11). Although the compositions of the displaced residual liquids are not known and probably changed as the zone of crystallization progressed upward, reasonable compositions more silicic than the residual liquid at the time each rock formed can produce similar results with different amounts.

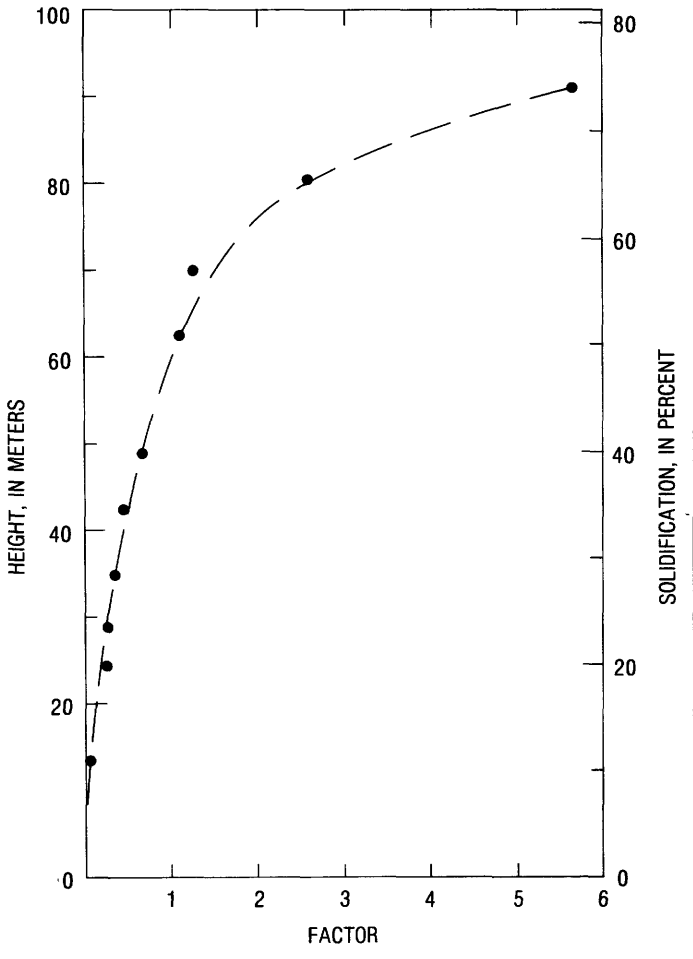

Figure 11. Proportion (factor) of liquid with composition of average silicic zone rock that added to rock duplicates composition of residual liquid (see table 6).

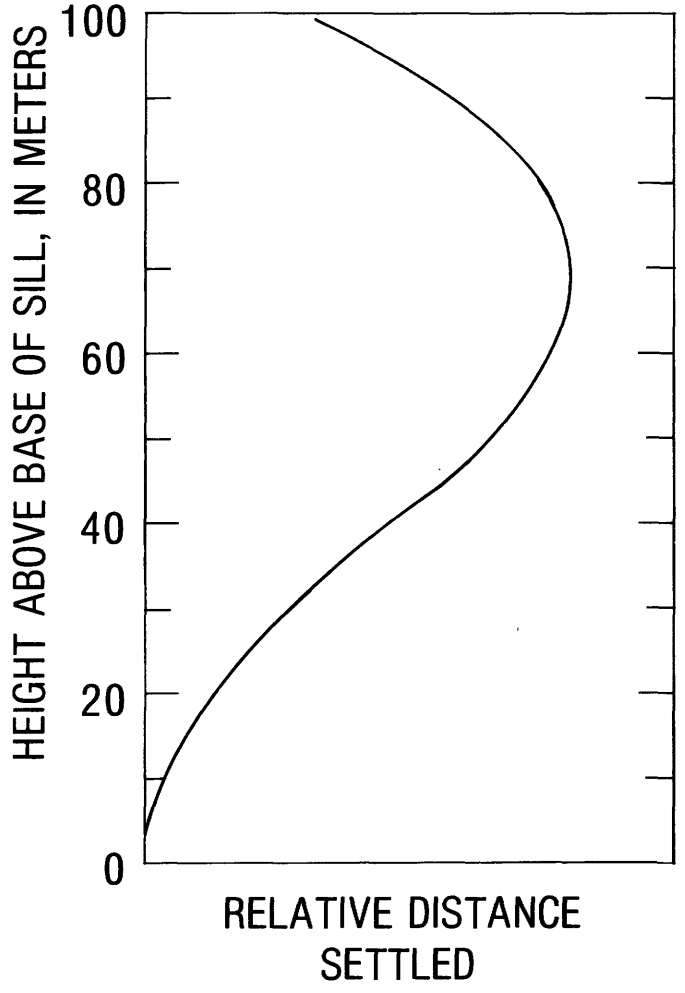

Figure 12. Relative distance that olivine could settle as a function of height within sill. As crystallization zone moved upward it became progressively thicker allowing more time for settling. Late decrease in settling rate results from increasing viscosity of residual liquid.

The relative distances that crystals of olivine could settle within the crystallization zone as a function of height above the base of the sill are shown in figure 12. At progressively greater height, the zone of crystallization would be progressively thicker, and thus more time would be available for individual crystals to settle. Thus, the efficacy of settling increases as the zone moves upward and as its thickness increases. At the last stage of formation of the lower gabbro the effect of settling decreases as the increasing viscosity of the bulk residual magma in the interior begins to have a strong influence on settling rate. Although the curve shown is based on calculated distances of settling, no scale for distance is shown on figure 12 because no data are available on the probable temperature interval over which olivine would have been on the liquidus. For simplification in the calculation, the bounding isotherms were assumed to remain the same, whereas they actually would have decreased upward as the bulk liquid became more silicic.

The loss of relatively silicic residual liquid (displaced upward) and the addition of settled crystals would cause the bulk composition (crystals plus remaining liquid) of the lower part of the crystallization zone to be more refractory. Therefore, the crystals would have a more refractory composition when crystallization was completed at successive intervals than if no settling had occurred. Such an upward increase in refractory components of minerals is shown by the upward increase in Mg/Fe in olivine and ferroaugite, the slight absolute increase in Ca/Na in plagioclase, and the increase in Mg/Fe and Ca/Na of rocks from the base toward the center of the sill. As the rocks became progressively more mafic, the bulk residual magma became more silicic.

If crystallization zone settling was the major

process of differentiation of the gabbro sill, the residual magma, displaced by settling crystals, must have been mixed with overlying magma. The displaced residual liquid would have had a lower density (more silicic composition) than the overlying, probably convecting, magma and thus may have risen buoyantly and have been homogenized with it. If the displaced residual liquid was not mixed, but settling still occurred, a strong chemical gradient would have been locally established and chemically graded rhythmic layers probably would have been produced (Jackson, 1961, p. 94–98).

The upper zone of crystallization progressed continuously but slowly downward during solidification of the sill (fig. 8). In contrast to the lower zone, settling in this upper zone would result in removal of crystals from the zone. These crystals would sink toward the interior of the sill into magma hotter than in the upper zone of crystallization where they formed. Therefore, the settled crystals would be progressively resorbed during their downward transport if sufficient heat was available.

Heat released in the upper zone by crystallization would be removed from the interior of the sill by resorption. Thus crystallization, settling, and resorption probably would produce a net upward transport of heat, and as a result, high temperatures would be maintained near the top of the sill, causing it to solidify less rapidly from the top than from the base (Irvine, 1970). This process would largely account for the smaller thickness of the upper compared to the lower gabbro zone. The crystals that settled from the upper zone would, upon being resorbed, add refractory components to the interior magma. At the top of the upper zone of crystallization, the residual magma would have an increased viscosity (cooler and more silicic as a result of downward settling of early minerals) and settling would be impeded; thus this zone would move slowly downward.

If the crystals that settled downward from the upper crystallization zone had not been resorbed in the interior, but had settled through the sill into the lower zone of crystallization, a rhythmic layering or sharp increase in minerals with a high settling rate (for example, olivine) would be expected in the lower part of the sill. No such rhythmic layering or marked increase in any of the early minerals was observed. In addition, the first crystals to settle through the sill to the bottom would have had the more refractory composition, but no such compositions are found in the lowest part of the sill. Indeed, the most refractory mineral compositions occur near the center of the sill.

Because the upper zone progressed downward much less rapidly than the lower zone moved upward, the displaced silicic residual magma accumulated high in the sill where it formed the rocks of silicic zone. The variations exhibited by rocks in the silicic zone most likely are the result of several processes including filter pressing (compaction of crystal mush), crystal settling, and possibly alkali diffusion. Crystal settling would have been much less efficient in producing compositional changes in the magma in this zone because viscosity was much greater (more silicic magma) than at an earlier stage when the lower gabbro zone was formed. Transgressive ferrogranophyre and granophyre bodies probably are the products of magma that was filter pressed from a somewhat lower part of the silicic zone (where the last part of the sill, other than the transgressive bodies, crystallized). The magma was injected into the upper part of the silicic zone and in places into the upper gabbro zone, perhaps along vertical and horizontal joints. The wide variation in Na_2O/K_2O in the granophyres, whose composition is otherwise similar, suggests that alkali diffusion may have occurred during the last stages of crystallization.

SUMMARY

Crystal settling in zones of crystallization that moved inward from the margins of the Stott sill as it solidified appears to account for the variation in mineralogy and petrochemistry in the sill. In the lower zone of crystallization, the amount of settled individual minerals was controlled by their height of nucleation and settling rate. Viscosity increased downward so that settling rates were very low near the base of the zone and no well-defined floor was present. Thus lamination or layering was not produced. The amount of settling increased as the zone moved upward because the zone became increasingly thicker and more time was available for settling. Liquid displaced upward by settled crystals was probably homogenized with magma in the interior of the sill. Crystals in the upper zone of crystallization settled downward into the interior of the sill where they were resorbed. As a result of the effects of heat of crystallization and resorption, high temperatures were maintained in the upper part of the sill, and the upper crystallization zone moved downward much more slowly than the lower crystallization zone moved upward. Thus the last part of the sill to solidify was in the upper part.

Differentiation by settling in zones of crystallization should be particularly pronounced where the constituent minerals crystallize over a wide temperature range. Such a wide temperature range may be

much more important for this type of differentiation than thickness of the sill and consequent greater time of solidification. Also important is the magma viscosity because of its effect on settling rate. Other sills much thicker than the Stott sill may have undergone a similar history but show much smaller degrees of fractionation.

REFERENCES CITED

Baldwin, E. M., 1955, Geology of the Mary's Peak and Alsea quadrangles, Oregon: U.S. Geological Survey Oil and Gas Investigations Map OM-162, scale 1:62,500.

_____ 1964 Geology of the Dallas and Valsetz quadrangles, Oregon: Oregon Department of Geology and Minerals Industries Bulletin 35 (revised), 56 p.

Barlett, R. W., 1969, Magma convection, temperature distribution, and differentiation: American Journal of Science, v. 267, p. 1067-1082.

Bottinga, Y., and Weill, D. F., 1970, Densities of liquid silicate systems calculated from partial molar volumes of oxide components: American Journal of Science, v. 269, p. 169-182.

Brown, G. M., and Vincent, E. A., 1963, Pyroxenes from the late stages of fractionation of the Skaergaard intrusion, east Greenland: Mineralogical Magazine, v. 32, p. 511-543.

Campbell, I. H., 1978, Some problems with the cumulus theory: Lithos, v. 11, p. 311-323.

Carmichael, I. S. E., 1960, The pyroxenes and olivines from some Tertiary acid glasses: Journal of Petrology, v. 1, p. 309-336.

Clark, H. C., 1969, Remnant magnetization, cooling history, and paleomagnetic record of the Marys Peak sill, Oregon: Journal of Geophysical Research, v. 74, p. 3143-3160.

De, Aniruddha, 1974, Silicate liquid immiscibility in the Deccan traps and its petrogenetic significance: Geological Society of America Bulletin, v. 85, p. 471-474.

Ernst, W. G., 1966, Synthesis and stability relations of ferrotremolite: American Journal of Science, v. 264, p. 37-65.

Hess, H. H., 1960, Stillwater Igneous Complex, Montana: Geological Society of America Memoir 80, 230 p.

Irvine, T. N., 1970, Heat transfer during solidification of layered intrusions—1, sheets and sills: Canadian Journal ofEarth Sciences, v. 7, no. 4, p. 1031-1061.

_____1975, The silica immiscibility effect of magmas: Carnegie Institute of Washington Year Book 1974-1975, p.484-492.

Jackson, E. D., 1961, Primary textures and mineral associations in the ultramafic zone of the Stillwatercomplex, Montana: U.S. Geological Survey Professional Paper 358, 106 p.

_____1971, The origin of ultramafic rocks by cumulus processes: Mineralogical Magazine, v. 48, p. 138-174.

Jaeger, J. C., 1957, The temperature in the neighborhood of a cooling intrusive sheet: American Journal of Science, v. 255, p. 306-318.

Lindsley, D. H., and Munoz, J. L., 1969, Subsolidus relationships along the join Hendenbergite-Ferrosilite: American Journal of Science, v. 267A, p. 295-324.

McBirney, A. R., 1975, Differentiation of the Skaergaard intrusion: Nature, v. 253, p. 691-694.

McBirney, A. R., and Nakamura, Yasuo, 1974, Immiscibility in late-stage magmas of the Skaergaard intrusion: Carnegie Institute of Washington Year Book 1973-1974, p. 348-352.

McDougall, Ian, 1961, Optical and chemical studies of pyroxenes in a differentiated Tasmanian dolerite: American Mineralogist, v. 46, p. 661-687.

MacLeod, N. S., 1969, Geology and igneous petrology of the Saddleback area, central Oregon Coast Range: Santa Barbara, University of California, Ph. D. thesis, 205 p.

Richter, D. H., and Moore, J. G., 1966, Petrology of Kilauea-Iki lava lake, Hawaii: U.S. Geological Survey Professional Paper 537-B, 26 p.

Roberts, A. E., 1953, A petrographic study of the intrusive at Marys Peak, Benton County, Oregon: Northwest Science, v. 27, no. 2, p. 43-60.

Roedder, Edwin, 1951, Low-temperature liquid immiscibility in the system K_2O-FeO-Al_2O_3-SiO_2: American Mineralogist, v. 36, p. 282-286.

Shaw, H. R., 1972, Viscosities of magmatic silicate liquids—an empirical method of prediction: American Journal of Science, v. 272, p. 870-890.

Smith, Douglass, 1971, Reconnaissance experiments with compositions on the join $Fs_{88}En_{15}$-wollastonite in the pyroxene quadrilateral: Carnegie Institute of Washington Year Book, 1970-1971, p. 125-129.

Snavely, P. D., Jr., and Wagner, H. C., 1961, Differentiated gabbroic sills and associated alkalic rocks in the central part of the Oregon Coast Range, Oregon, *in* Geological Survey Research 1961: U.S. Geological Survey Professional Paper 424-D, p. D156-D161.

Snavely, P. D., Jr., MacLeod, N. S., and Wagner, H. C., 1968, Tholeiitic and alkalic basalts of the Eocene Siletz River Volcanics, Oregon Coast Range: American Journal of Science, v. 266, p. 454-481.

Snavely, P. D., Jr., MacLeod, N. S., and Rau, W. W., 1969, Geology of the Newport area, Oregon: Ore Bin, v. 31, nos. 2 and 3, p. 25-71.

Snavely, P. D., Jr., MacLeod, N. S., Wagner, H. C., and Rau, W. W., 1976, Geologic map of the Cape Foulweather and Euchre Mountain quadrangles, Oregon: U.S. Geological Survey Miscellaneous Investigations Series Map I-868, scale 1:62,500.

Tatsumoto, M., and Snavely, P. D., Jr., 1969, Isotopic composition of lead in rocks of the Coast Range, Oregon and Washington: Journal of Geophysical Research, v. 74, p. 1087-1100.

Uruno, K., 1963, Optical study of the ordering degree of plagioclase: Tohoku University Science Reports, 3d series, v. 8, no. 2, p. 171-220.

Wager, L. R., 1960, The major element variations of the layered series of the Skaergaard intrusion [Greenland] and a reestimation of the average composition of the hidden layered series and of the successive residual magmas: Journal of Petrology, v. 1, no. 3, p. 364-398.

Wager, L. R., and Brown, G. M., 1968, Layered igneous rocks: Edinburgh and London, Oliver and Boyd, 588 p.

Wilshire, H. G., 1967, The Prospect alkaline diabase-picrite intrusion, New South Wales, Australia: Journal of Petrology, v. 8, p. 97-163.

Yoder, H. S., Jr., and Sahama, T. G., 1957, Olivine X-ray determinative curve: American Mineralogist, v. 42, p. 475-491.